2007

Contrasting Biogeochemistry of Six Trace Metals during the Rise and Decay of a Spring Phytoplankton Bloom in San Francisco Bay

Allison C. Luengen
University of San Francisco, aluengen@usfca.edu

Peter T. Raimondi

A. Russell Flegal

Limnol. Oceanogr., 52(3), 2007, 1112–1130

Contrasting biogeochemistry of six trace metals during the rise and decay of a spring phytoplankton bloom in San Francisco Bay

Allison C. Luengen[1]
Environmental Toxicology Department, WIGS Group, University of California at Santa Cruz, 1156 High Street, Santa Cruz, California 95064

Peter T. Raimondi
Ecology and Evolutionary Biology Department, University of California at Santa Cruz, 1156 High Street, Santa Cruz, California 95064

A. Russell Flegal
Environmental Toxicology Department, WIGS Group, University of California at Santa Cruz, 1156 High Street, Santa Cruz, California 95064

Abstract

The spring 2003 phytoplankton bloom in South San Francisco Bay (South Bay) affected the cycling of Mn, Co, Zn, Ni, and Pb, but not Cu. We followed this diatom bloom for 2 months, capturing a peak in chlorophyll *a* (Chl *a*) of >150 μg L^{-1} and then an increase in dissolved organic carbon of >400 μmol L^{-1} as phytoplankton decomposed. To determine how the stages of the bloom affected metal concentrations, we used principal component analysis to reduce our 15 water chemistry variables into a bloom factor, a sorbent factor, and a decay factor. Increasing values of the bloom factor, which was a composite of dissolved oxygen, Chl *a*, and other variables, significantly accounted for reductions in dissolved Mn, Ni, and Pb. We attributed those declines to microbial oxidation, phytoplankton uptake, and sorption onto phytoplankton, respectively. In contrast, dissolved Cu concentrations were not explained by either the bloom or decay factors, consistent with previous studies showing its strong organic complexation and limited bioavailability in South Bay. The decay factor significantly accounted for increases in dissolved Mn, Co, Zn, and Pb. Decomposing bloom material presumably caused suboxic conditions in surface sediments, resulting in release of metals to overlying waters during reductive dissolution of Mn and Fe (hydr)oxides. These alterations in metal cycling during a nutrient-enriched bloom were evidence of eutrophication. Annually, phytoplankton productivity has the potential to affect metal retention in the estuary; in 2003, 75% of Ni discharged into lower South Bay by wastewater treatment plants was cycled through phytoplankton.

Metal contamination and eutrophication, or biological changes that result from excessive nutrient inputs, are two interrelated problems affecting many estuaries, including San Francisco Bay (Cloern 2001; Flegal et al. 2005). The Bay (Fig. 1), which is one of the largest estuaries on the western coast of North America, is an ideal field site to investigate the interaction between metal cycling and phytoplankton blooms for several reasons. The southern reach of the estuary (South Bay) is contaminated with trace metals, including Co, Zn, Cu, Ni, and Pb (Flegal et al. 2005). The South Bay also has a predictable, nutrient-enriched spring phytoplankton bloom, which has been well characterized (Cloern 1996). During the bloom, phytoplankton can take up some metals, thereby increasing metal bioavailability to the food chain and trapping those metals within the estuary (Lee and Luoma 1998; Luoma et al. 1998).

South Bay has seasonally high concentrations of many trace metals (Flegal et al. 1991). Metals such as Co, Ni, Cu, Zn, and Pb are elevated as a result of diagenetic remobilization from contaminated sediments (Rivera-Duarte and Flegal 1997; Squire et al. 2002) and desorption from resuspended sediments (Gee and Bruland 2002). Metal concentrations typically peak in summer, when freshwater flow from the Sacramento and San Joaquin Rivers is low (Flegal et al. 1991). Those rivers empty into the northern reach of the estuary (Fig. 1) and

[1] Corresponding author (luengen@etox.ucsc.edu).

Acknowledgments

Jim Cloern, U.S. Geological Survey (USGS), and his lab group, including Amy Little, Cary Burns Lopez, and Tara Schraga, provided the shipboard measurements and boat time that made this project possible. We thank the crew of the R/V *Polaris*, and we thank Steve Hager, USGS, for his nutrient analyses. Jeanne DiLeo, USGS, contributed the map used in Fig. 1. Rob Franks, University of California at Santa Cruz (UCSC), provided invaluable assistance with ICP-MS and ICP-OES. Sara Tanner, Moss Landing Marine Laboratories, analyzed the dissolved organic carbon samples. Richard Looker, California Regional Water Quality Control Board, supplied wastewater treatment plant data. Helen Cole, UCSC, assisted with the graphics. We thank members of the WIGS group at UCSC for help with collecting and preparing samples, particularly Christopher Conaway, Sharon Hibdon, Mari Gilmore, and Genine Scelfo. We are grateful to Raphael Kudela and Ken Bruland, UCSC, and Sam Luoma, USGS, for their many comments on methods and drafts. We thank Kristen Buck, UCSC, and two anonymous reviewers for valuable comments on the manuscript.

The University of California Center for Water Resources partially funded this project.

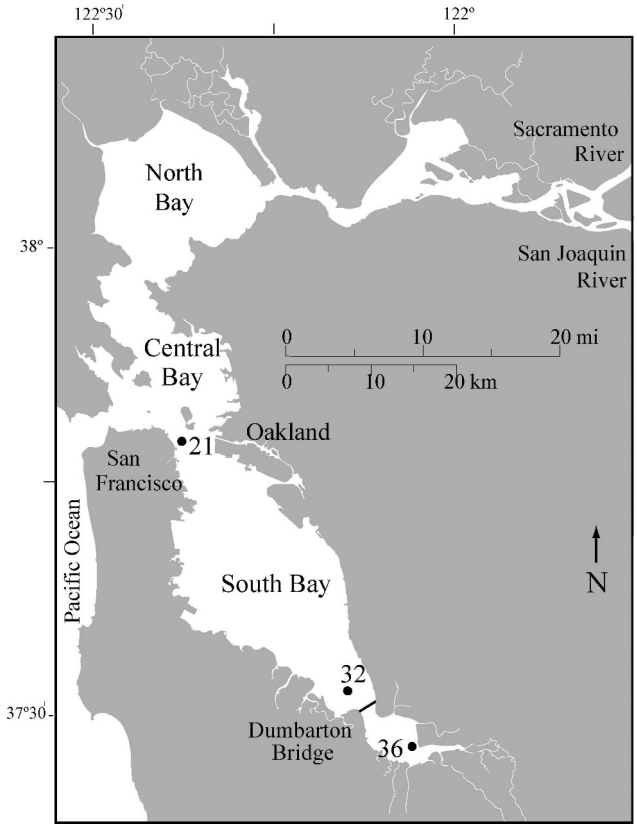

Fig. 1. The USGS stations in South San Francisco Bay (South Bay) that we sampled during this study were site 21 (Bay Bridge), site 32 (Ravenswood Point), and site 36 (Calaveras Point).

exchange with South Bay only during periods of high river flow.

Although South Bay has elevated metal concentrations, the bioavailability of some metals can be limited by complexation to organic ligands, as described in the free ion model developed by Sunda and Huntsman (1998). In that model, the free metal ion (e.g., Cu^{2+}) is the form equilibrating with cellular receptors. Metals complexed to charged organic ligands do not dissociate rapidly enough for the free metal ion to be complexed to receptor sites and then transported into the cell (Sunda and Huntsman 1998). Thus, most organically complexed metals are not readily bioavailable to phytoplankton. For example, Cu is strongly complexed to organic ligands in South Bay (Buck and Bruland 2005; Hurst and Bruland 2005). As a result of that complexation, dissolved Cu was not depleted from South Bay water by a spring bloom in 1994 (Luoma et al. 1998) or by a laboratory simulation of the South Bay bloom (Beck et al. 2002).

The South Bay bloom occurs predictably every spring (February–April), although its timing and magnitude vary annually on the basis of freshwater input, winds, tides, and nutrient concentrations (Cloern 1996). In early spring, freshwater input and warm, calm weather stratify the water column and create conditions for the bloom by isolating phytoplankton from benthic grazers and increasing light exposure (Cloern 1996). The bloom is dominated by diatoms, including *Thalassiosira rotula, Thalassiosira hendeyi, Thalassiosira punctigera, Chaetoceros socialis, Chaetoceros debilis, Skeletonema costatum, Ditylum brightwellii*, and *Coscinodiscus oculus-iridis* (Cloern and Dufford 2005). The bloom typically occurs during neap tides when reduced mixing both helps maintain stratification and prevent phytoplankton from being advected out of the estuary. The magnitude of the bloom may also be affected by the amount of nutrients, which have elevated concentrations in the heavily urbanized South Bay as a result of wastewater treatment plant inputs (Hager and Schemel 1996). Previous phytoplankton blooms in South Bay have been observed to crash after depletion of nutrients from the water (Hager and Schemel 1996; Grenz et al. 2000).

Along with nutrients, trace metals have also been depleted by blooms in South Bay (Luoma et al. 1998), the Scheldt estuary (Zwolsman and van Eck 1999), coastal waters (Schoemann et al. 1998; Ingri et al. 2004), and laboratory mesocosm studies (Beck et al. 2002; Riedel and Sanders 2003; Wang et al. 2005). In South Bay, the 1994 spring bloom depleted dissolved Cd, Ni, and Zn (but not Cu) from the water (Luoma et al. 1998). Similarly, Zwolsman and van Eck (1999) observed a depletion of dissolved Cd and Zn^{-} but not Cu^{-} during a bloom in the Scheldt estuary. Studies in coastal waters have shown that metals (e.g., Mn or Fe) can then be remobilized as blooms decay (Thamdrup et al. 1994; Schoemann et al. 1998). However, the number of such studies is limited by both the difficulty of capturing a bloom in the field and attributing any observed changes in metal concentrations to bloom processes (Luoma et al. 1998). Because of these difficulties, some researchers have used mesocosm studies (Beck et al. 2002; Riedel and Sanders 2003; Wang et al. 2005) or large field enclosures (Muller et al. 2005) to study the effect of phytoplankton blooms on metal concentrations.

In addition to previous bloom studies, we used the oceanic distributions of our trace elements to determine how the metals were likely to be affected by bloom processes. For example, the oceanic profile of dissolved Mn is shaped by geochemical scavenging and redox activity (Bruland et al. 1991). Maximum concentrations of dissolved Mn in surface waters are maintained by photoreduction of manganese oxides and photoinhibition of bacteria, which oxidize dissolved Mn to particulate Mn (Sunda and Huntsman 1988). On the basis of this cycling of Mn between dissolved and particulate forms and a past study (Beck et al. 2002) indicating that bacteria can oxidize dissolved Mn during South Bay blooms, we expected that dissolved Mn would by depleted by microbial oxidation during our bloom. Because Co is oxidized by the same microbial pathway as dissolved Mn (Moffett and Ho 1996), we also hypothesized that dissolved Co would be depleted by bacterial oxidation.

On the basis of the oceanic distributions of Zn, Ni, and Pb, we hypothesized that those metals would also be depleted during a phytoplankton bloom. Both Zn and Ni have nutrient-type distributions characterized by depletion in surface oceanic waters as a result of phytoplankton uptake (Bruland and Lohan 2004). We expected those two

metals to be assimilated by phytoplankton during our bloom, unless they were highly complexed to organic ligands. In contrast, because Cu is strongly complexed in South Bay (Buck and Bruland 2005), we hypothesized that the bloom would not deplete that metal from the water. Finally, because Pb is a scavenged-type element (Kozelka et al. 1997; Bruland and Lohan 2004), we hypothesized that it would decrease because of sorption to phytoplankton.

For those metals that were likely to be depleted by the bloom (Mn, Co, Zn, Ni, and Pb), we developed quantitative hypotheses to determine how much metal could be taken up by a theoretical bloom that reached 65 μL^{-1} of chlorophyll *a* (Chl *a*). A bloom of that magnitude (which was the average Chl *a* at our sites 32 and 36) would result in a decrease of 0.19 mmol C L^{-1} in water, given a [C] : [Chl *a*] ratio of 35 (Cloern et al. 1995), as shown below:

$$\left(\frac{65\ \mu\text{g Chl } a}{\text{L}}\right)\left(\frac{35\ \mu\text{g C}}{\mu\text{g Chl } a}\right)\left(\frac{1\ \text{mol C}}{12\ \text{g C}}\right) = \frac{0.19\ \text{mmol C}}{\text{L}}$$

By multiplying 0.19 mmol C L^{-1} by [metal] : [C] ratios, we calculated the potential depletion of each metal by phytoplankton during the bloom (Table 1). Then, to determine how the bloom affected those metals, we collected water samples at weekly intervals from mid-February to the beginning of May.

By combining frequent field sampling with principal component analysis (PCA), we were able to address the challenge of following the biogeochemical cycling of metals during a bloom in the field. With these approaches, we sought to (1) distinguish the effect of bloom growth versus decay, (2) determine whether the bloom depleted dissolved Ni given previous conflicting results (Luoma et al. 1998; Beck et al. 2002) regarding the bioavailability of Ni in the South Bay, (3) make the first measurements of Co and Pb during a South Bay bloom, and (4) contrast the cycling of these metals to elucidate their differing biogeochemistries. To explore these objectives, we focused on representative metals with nutrient, scavenged, and hybrid profiles (Bruland and Lohan 2004; Morel et al. 2004) and different degrees of organic complexation.

Methods

Sampling design—Water samples were collected at three sites in the central channel of South Bay (Fig. 1) during cruises designed to capture the spring 2003 phytoplankton bloom. During the first cruise on 19 February, all parameters shown in Table 2 were measured, except dissolved organic carbon (DOC). Beginning 24 February, all parameters listed in Table 2, as well as dissolved (<0.45 μm) and total (unfiltered) trace metals, were measured. Cruises on 24 February, 04 March, 12 March, and 27 March captured trace metal concentrations and associated water chemistry during a period of high phytoplankton biomass. The 01 April, 17 April, 23 April, and 01 May cruises traced the decline of the bloom. The 27 August cruise was timed to provide a low phytoplankton

Table 1. Potential algal drawdown of each metal (Me) from the water column on the basis of a bloom of 65 μg L^{-1} Chl *a*, a depletion of 5.16 nmol L^{-1} P, and [Me] : [C] and [Me] : [P] ratios for phytoplankton. By using Monterey Bay and Southern Ocean phytoplankton data to calculate the potential depletion of metals by our bloom, we were able to estimate how much of our observed changes in metal concentrations (average of sites 32 and 36) could be explained by phytoplankton assimilation. When our changes in dissolved metal concentrations far exceeded those predicted for phytoplankton activity (e.g., Mn), we considered other processes (e.g., diagenetic remobilization from sediments).

	Monterey Bay phytoplankton*		High-Fe Southern Ocean diatoms†		Potential algal drawdown calculated from		Highest–lowest average dissolved Me concentration (nmol L^{-1})‡	Possible contribution of phytoplankton to Me concentration (%)‡
					Me : C	Me : P		
Element	Me : P (mmol mol^{-1})	Me : C (μmol mol^{-1})	Me : P (mmol mol^{-1})	Me : C (μmol mol^{-1})	(nmol L^{-1})	(nmol L^{-1})		
Mn	0.39	3.7	0.28	4.5	0.70–0.86	1.4–2	1,600	0.04–0.1
Co	<0.07	<0.6			<0.1	<0.4	4.0	3–10
Zn	0.84	7.9	6.2	71	1.5–13	4.3–32	15	10–100
Cu	0.18	1.7			0.32	0.93	No change	—
Ni	0.21	2.0	0.73	8.5	0.38–1.6	1.1–3.8	5.8	7–70
Pb	0.04	0.3			0.06	0.2	0.08	70–100

* Martin and Knauer 1973. Martin and Knauer (1973) collected Monterey Bay phytoplankton samples during a diatom bloom in conditions where suspended sediment concentrations were low. To further minimize contamination by suspended sediments, Bruland et al. (1991) selected Mn, Zn, Cu, and Ni data from that study for low Al concentrations. Following Bruland's protocol, we selected data for Co and Pb. Lead is shown for the one low-Al sample in which it was detected, and Co is shown as less than the detection limit.

† Twining et al. 2004. We used phytoplankton data from the Southern Ocean (Twining et al. 2004) because the authors measured metal concentrations in individual cells, which eliminated the suspended sediments that often confounded other field studies.

‡ This study.

Table 2. Parameters measured during the spring 2003 bloom.

Variable	Explanation
Chl *a*	Chl *a* measured from discrete sample
Phaeo	Phaeophytin measured from discrete sample
Chl ratio	Chl *a*/(Chl *a* + Phaeo)
SPM	Suspended particulate matter calculated from optical backscatter
Salinity	Salinity
DO	Percentage of dissolved oxygen that would be present if in atmospheric equilibrium
T	Temperature
σ_t	Water density
DOC	Dissolved organic carbon
DRP	Dissolved reactive phosphate
DSi	Dissolved silicate
DIN	Dissolved inorganic nitrogen (nitrate, nitrite, and ammonium)
UFFe	Total (unfiltered iron)
UFMn	Total (unfiltered manganese)
Tide	Tidal amplitude

biomass contrast to the spring data. All samples were taken aboard the U.S. Geological Survey (USGS) R/V *Polaris*.

Vertical profiles of the water column were taken with a Sea-Bird Electronics (SBE) underwater unit (SBE-9 plus) according to established methods (Caffrey et al. 1998). The instrument package included SBE conductivity–temperature–depth (CTD) sensors, biospherical photosynthetically active radiation (PAR) light sensor, SCUFA fluorometer, SBE-43 dissolved oxygen sensor, and D&A Instruments optical backscatter for suspended particulate matter (SPM). The latter three sensors were calibrated each cruise with discrete samples (from 2 m depth via the ship's flow-through system) at six USGS sites, including sites 21, 32, and 36, where the samples for this study were collected. For Chl *a* discrete samples, duplicate aliquots were filtered onto GFF filters. The filters were then frozen immediately, stored at −80°C, acetone-extracted, and analyzed with a Turner TD700 fluorometer (Parsons et al. 1984). Dissolved oxygen (DO) samples were analyzed by Winkler titration (Granéli and Granéli 1991). SPM was measured by gravimetric analysis of samples collected onto 0.45-μm polycarbonate filters (Hager 1994).

Surface (1 m) water was collected with the use of two peristaltic pumps equipped with acid-cleaned Teflon tubing attached to an aluminum pole extended out from the boat, as per the methods that the WIGS group (University of California at Santa Cruz) had previously used in San Francisco Bay (Flegal et al. 1991). The metal samples were collected with clean techniques into 1-liter acid-cleaned low-density polyethylene bottles. Additional samples were collected for nutrients, DOC, Chl *a*, and phaeophytin (Phaeo). Filtered (0.45 μm) water for dissolved metals was obtained by attaching an acid-cleaned Osmonics polypropylene filter (Calyx Capsule) to the tubing of one pump. The second pump was used to collect unfiltered water for total metal samples.

Trace metal analyses—Trace metal samples (both dissolved and total) were acidified in the laboratory approximately 3 months before analysis by addition of 4 mL of 6 mol L^{-1} high-purity (Optima®) hydrochloric acid (HCl) to a 1-liter sample. A 30-mL aliquot of acidified sample was then ultraviolet (UV) digested (Ndung'u et al. 2003). Concentrations of Co, Cu, Ni, Zn, and Pb were measured by high-resolution inductively coupled plasma magnetic sector mass spectrometry (ICP-MS) with a Finnigan Element ICP-MS and a Finnigan microsampler, according to established methods (Ndung'u et al. 2003). These methods included an online preconcentration step with a chelating resin (AF-Chelate 650M) to concentrate and remove the metals from the saltwater matrix (Warnken et al. 2000). National Research Council Canada certified reference materials (CRMs) CASS-4, SLEW-2, and SLEW-3 for trace elements in water were used to quantify recoveries (Table 3).

Acidified (pH $<$ 1) samples were analyzed for dissolved and total Mn and total Fe by inductively coupled plasma optical emission spectrometry (ICP-OES) with a Perkin-Elmer 4300DV in radial mode. CRMs SLEW-2 and SLRS-1 were analyzed concurrently to quantify accuracy (Table 3).

Particulate metal concentrations were calculated as the difference between the total and dissolved samples. The

Table 3. Trace metal analyses figures of merit, showing mean ± 1 standard deviation.*

Element†	Material type	Co (nmol L^{-1})	Ni (nmol L^{-1})	Cu (nmol L^{-1})	Zn (nmol L^{-1})	Pb (nmol L^{-1})	Fe (nmol L^{-1})	Mn (nmol L^{-1})
DL (3σ)		0.048	2.0	0.21	0.56	0.001	43	7.1
CASS-4	Measured	0.39±0.02	4.9±0.6	9.5±0.3	6.9±0.5	0.050±0.005		
	Certified	0.44±0.03	5.35±0.26	9.32±0.43	5.83±0.44	0.047±0.009		
SLEW-2	Measured		13.1±0.9	26.8±1.0	19.5±0.9	0.11±0.02		298±2
	Certified		12.1±0.5	25.5±0.9	16.8±1.1	0.13±0.01		311±10
SLEW-3	Measured	0.76±0.03	21.8±0.6	26.4±0.4	2.5±0.3	0.035±0.005		
	Certified	0.71±0.08	21.0±0.6	24.4±0.9	3.07±0.28	0.043±0.003		
SLRS-1	Measured						633±32	32±1
	Certified						564±19	32±0.2

* All measured and certified values were within one standard deviation of each other, except SLEW-2 for Zn, SLEW-3 for Cu, and SLRS-1 for Fe. Those values were within two standard deviations of each other.

† DL, detection limit; CASS-4, SLEW-2, SLEW-3, and SLRS-1 are certified reference materials provided by the National Research Council of Canada for ocean water, estuarine water, and river water, respectively.

distribution coefficient, K_d, was then given as moles of particulate metal per gram of SPM divided by the concentration of dissolved metals. Accordingly, K_d values were given in units of liters per kilogram.

Nutrients and DOC—Dissolved reactive phosphate (DRP), dissolved inorganic nitrogen (DIN), and dissolved silica (DSi) were analyzed with a Technicon Autoanalyzer II, according to established colorimetric methods (Hager 1994). DIN was the sum of NO_3^-, NO_2^-, and NH_4^+. Most samples were frozen and thawed overnight before analysis.

DOC samples were analyzed with a Dohrmann DC-190 (Rosemount Anaytical, temperature 680°C, catalyst 0.5% $PtAl_2O_3$) according to established methods (Sharp et al. 1993). Typical precision was 2.5–4.5 μmol L^{-1} (SD) or 1–5% of the certified value. The detection limit was 2.9 μmol L^{-1}.

Data analyses—Results from the concurrent vertical profiles (e.g., Chl *a*, SPM, salinity) can be found on the USGS web site at http://sfbay.wr.usgs.gov/access/wqdata. Instrument results for SPM and DO were used rather than discrete samples because instrument data were available at 1 m, the depth at which the trace metal samples were collected. Results from discrete Chl *a* samples collected from the peristaltic pump were used in the data analyses instead of USGS discrete or instrumental data.

An additional variable, tidal amplitude, was calculated with data from Yerba Buena Island, Dumbarton Bridge, and Calaveras Point corresponding to sites 21, 32, and 36 from WWW Tide and Current Predictor (http://tbone.biol.sc.edu/tide/). On the basis of the time at which samples were collected, tidal amplitude was calculated as the absolute value of the difference between the nearest high and low tide. Then, outgoing tides were given a negative value and incoming tides a positive value for statistical analyses.

PCA—To address the challenge of characterizing the bloom in the field, we employed PCA (with Systat Version 10.2.05, SPSS) to develop composite factors that described bloom processes. A similar approach was used by Osenberg et al. (1992) to derive factors that described the spatial variability of infaunal taxa in relation to distance from a produced water outfall. We first log-transformed SPM, DOC, DRP, Chl *a*, and Phaeo to satisfy assumptions of normal statistics. Then we used PCA to reduce the 15 variables (Table 2) to a bloom factor, a sorbent factor, and a decay factor (Table 4). The correlation between original variables and derived factors was given by the component loadings (Table 4). Original variables with component loadings ≥ 0.6 or ≤ -0.6 were interpreted according to Tabachnick and Fidell's (2001) discussion of cutoffs for loadings.

General linear models—To determine whether the three PCA factors and the categorical variable (site) affected dissolved metal concentrations, an analysis of covariance (ANCOVA) was performed with a general linear model (GLM) routine. These analyses illustrate the power of PCA in GLMs because all factors are, by definition, independent. In contrast, original variables are commonly collinear, which would violate assumptions of any GLM model. All dissolved metals were normally distributed, except Mn and Zn. Those two dependent variables were square root and log transformed, respectively. With the use of GLMs, the four-way interaction between the categorical variable (site) and the three covariates (PCA factors) was tested for homogeneity of surfaces and removed when its probability was >0.05.

Table 4. Three PCA factors were formed by the water chemistry variables. The water chemistry variables that composed each factor are listed and their loadings are given in parentheses.

Bloom factor*	Sorbent factor†	Decay factor‡
DO(0.703)	log SPM(0.748)	log DOC(−0.657)
T(−0.622)	σ_t(−0.646)	log Phaeo(0.697)
Salinity(−0.620)	log DRP(0.832)	
DIN(−0.607)	UFFe(0.819)	
DSi(−0.834)	UFMn(0.775)	
log Chl *a*(0.864)		

* High values of the bloom factor corresponded to high values of both Chl *a* and DO and low values of DIN, DSi, *T*, and salinity. Those low *T* and salinity values were probably the result of cold freshwater from fluvial inputs.

† High values of the sorbent factor characterized high concentrations of SPM, DRP (which is particle reactive), and Fe and Mn (hydr)oxides. Additionally, the sorbent factor included water density, which was inversely related to that factor likely because fluvial inputs contained high particulate concentrations.

‡ Decreasing values of the decay factor corresponded with increasing DOC concentrations, as phytoplankton were remineralized, and declining Phaeo concentrations.

A model-building approach was used to select models that were most predictive of dissolved metal concentrations and that used the fewest number of variables. In that approach, we ran backward models that first included all three covariates and the categorical variable, site. Variables with $p > 0.15$ were then successively dropped. The r^2 values from different models were also used to assess the effect of dropping variables. In some models, site, the only categorical variable, was removed, and GLMs were then used to perform multiple linear regression. In the final models (Table 5), mean square errors or *t* values were used as estimates of the relative contribution of different factors.

A model-building approach was also used to determine the best predictors of distribution coefficients (K_d values) for all metals except Mn. Because total Mn was incorporated into the sorbent factor, we could not look at the effect of the PCA factors on Mn partitioning. Our model-building approach used both backward and forward models. In contrast to backward models that sequentially remove variables, forward models successively add variables. When the forward and backward models did not converge, the model with the highest r^2 value was selected (Table 6).

Resulting models often contained multiple predictor variables. To graphically represent multiple linear regression results for dissolved metals, we ran the model with all but one of the factors and then plotted the residuals against the missing factor (partial residual plots). We repeated this

Table 5. Reduced models for dissolved metal concentrations. These results were generated by running general linear models with the categorical variable (site) and the three PCA factors (bloom, sorbent, and decay). Then, a model-building approach was used to reduce the models to include only the independent variables that best predicted dissolved metal concentrations.*

Effect	Coefficient	SE	Std Coef	Tolerance	*t*	*p* (two-tail)
Reduced model for square root Mn $r^2 = 0.72$						
Constant	0.607	0.044	0.000		13.8	<0.01
Sorbent factor	0.245	0.045	0.582	1	5.46	<0.01
Decay factor	−0.255	0.045	−0.605	1	−5.68	<0.01
Bloom factor	−0.090	0.045	−0.213	1	−2.00	0.058
Reduced model for Co $r^2 = 0.77$						
Constant	4.10	0.194	0.000		21.2	<0.01
Sorbent factor	1.39	0.198	0.697	1	7.04	<0.01
Decay factor	−1.08	0.198	−0.538	1	−5.44	<0.01
Reduced model for log Zn $r^2 = 0.66$						
Constant	0.927	0.028	0.000		33.5	<0.01
Sorbent factor	0.107	0.028	0.463	1	3.78	0.001
Decay factor	−0.153	0.028	−0.664	1	−5.43	<0.01
Reduced model for Pb, $r^2 = 0.93$						
Constant	0.135	0.00492	0.000		27.4	<0.01
Sorbent factor	0.049	0.00501	0.547	1	9.79	<0.01
Decay factor	−0.068	0.00501	−0.758	1	−13.5	<0.01
Bloom factor	−0.022	0.00501	−0.240	1	−4.30	<0.01
Source	Sum of squares	df	Mean square	*F*-ratio	*p*	
Reduced model for Cu $r^2 = 0.86$						
Site	3247	2	1623	69.4	<0.01	
Decay factor	114	1	114	4.88	0.038	
Error	515	22	23.4			
Reduced model for Ni, $r^2 = 0.92$						
Site	1742	2	871	98.5	<0.01	
Decay factor	36.9	1	36.9	4.18	0.054	
Bloom factor	261	1	261	29.5	<0.01	
Error	186	21	8.84			

* Std Coef, standard coefficient; df, degrees of freedom.

Table 6. Reduced models for K_d, the distribution coefficient between the dissolved and solid phases. A model-building approach that included both forward and backward stepwise approaches was used to generate these reduced models.*

Source	Sum of-squares	df	Mean square	*F*-ratio	*p*	
Reduced backwards model for log Co K_d, $r^2 = 0.55$						
Site	1.05	2	0.525	12.7	<0.01	
Error	0.865	21	0.0412			
Reduced backward model for log Cu K_d, $r^2 = 0.45$						
Site	2.68	2	1.34	8.42	0.002	
Error	3.34	21	0.159			
Reduced forward model for log Ni K_d, $r^2 = 0.63$						
Site	0.259	2	0.130	7.64	0.004	
Sorbent factor	0.0761	1	0.0761	4.49	0.049	
Decay factor	0.108	1	0.108	6.37	0.022	
Bloom factor	0.0481	1	0.0481	2.84	0.110	
Error	0.288	17	0.0170			
Reduced backward model for log Pb K_d, $r^2 = 0.73$						
Site	0.963	2	0.481	17.7	<0.01	
Decay factor	0.118	1	0.118	4.36	0.051	
Bloom factor	0.160	1	0.160	5.90	0.026	
Error	0.489	18	0.027			
Effect	Coefficient	SE	Std Coef	Tolerance	*t*	*p* (two-tail)
Reduced forward model for log Zn K_d, $r^2 = 0.35$						
Constant	5.20	0.0389	0		133	<0.01
Sorbent factor	−0.0850	0.0379	−0.406	1	−2.24	0.036
Decay factor	0.0909	0.0396	0.415	1	2.30	0.033

* Std Coef, standard coefficient; df, degrees of freedom.

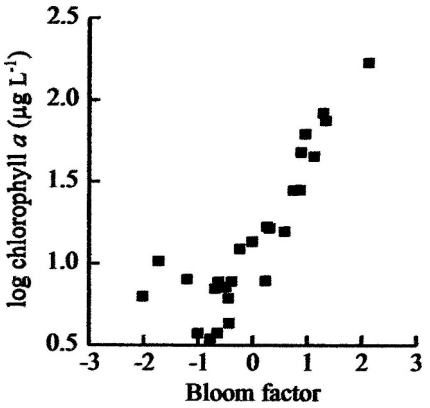

Fig. 2. The bloom factor was correlated with log Chl *a* (linear regression $F_{1,24} = 71$, $p < 0.01$, $r^2 = 0.75$).

process until each factor was individually plotted against the other sets of partial residuals. The resulting graphs showed how the omitted factor explained variation in the data and hence its contribution to the model. The slope of the relationship showed whether the factor negatively or positively affected metal concentrations. The relative contribution of the factors was indicated by the range of the *y*-axis, which showed the number of standard deviations of variation explained by that factor.

Results

PCA factors—The 15 water chemistry variables (Table 2) clearly separated into three PCA factors (Table 4). The separation of original variables into derived factors illustrates the utility of PCA for these types of analyses; groups of assorted original variables make up derived factors that often relate to ecological (or other) phenomena. The three derived factors collectively explained 77% of the variance.

The first PCA factor was a bloom factor, comprising log Chl *a* (+), DIN (−), DSi (−), DO (+), temperature (−), and salinity (−) (Table 4). The bloom factor was directly correlated with Chl *a*, our proxy for phytoplankton biomass (Fig. 2). However, it was a more complete representation of the rise of the bloom than Chl *a* alone because it included other variables.

The second PCA factor was a sorbent factor that represented the amount of particulate material, including SPM and Fe and Mn (hydr)oxides, available for metal sorption (Table 4). We use the term sorption to include metals that were adsorbed onto SPM, coprecipitated with Fe and Mn (hydr)oxides, or incorporated into organic matrices surrounding particles, as per Morel and Hering's (1993, p. 556) definition of sorption: "the partitioning of solutes between the solution and the whole of a particulate phase." In our sorbent factor, SPM and water density (σ_t) were inversely related, most likely because SPM increased with freshwater inputs that simultaneously decreased water density. DRP, which is particle reactive, also increased as SPM increased.

The third PCA factor was a decay factor. Declining values of that factor represented decomposition of phytoplankton. As the algae decayed, Phaeo decreased and DOC increased. The former was a particulate measure of Chl *a* breakdown, whereas the latter increased as organic material was remineralized into the dissolved phase.

Models describing metal concentrations—Table 5 shows which terms best explained the dissolved metal concentrations. Spatial terms (the categorical variable, site, or the sorbent factor) were part of the models for all metals. In many ways, the variable site and the sorbent factor modeled the same variance structure; the amount of particulates often accounted for the observed differences in metal concentrations between the sampling locations. However, the variable site predicted dissolved Ni and Cu concentrations better than the sorbent factor. Thus, some site-specific parameters not measured in this study contributed to variations in dissolved Ni and Cu concentrations.

The bloom factor accounted for variability in the concentrations of only three dissolved metals: Mn, Pb, and Ni (Table 5). The bloom factor did not affect dissolved Cu concentrations. That result was consistent with our hypothesis that organic complexation would limit algal uptake of dissolved Cu. Contrary to our hypothesis that Co and Zn would be depleted, concentrations of those two metals were not affected by the bloom factor. A subsequent discussion addresses three possible reasons for that lack of depletion.

The decay factor was an important variable governing concentrations of dissolved Mn, Co, Zn, and Pb, as demonstrated by the mean square error or *t* values (Table 5). Because the mean square error was an estimate of the variance attributable to the term of interest (e.g., the decay factor), it can be used to roughly assess the contribution of the term to the model fit. For example, in the dissolved Ni and Cu models, the relatively low mean square error indicated that the decay factor was comparatively unimportant relative to the other terms in those models. Similar to the mean square error, the *t* value indicated the variance explained by individual variables in a multiple linear regression model. In the dissolved Mn model, the *t* value for the decay factor was −5.68, whereas for the bloom factor, it was −2.00 (Table 5), indicating that the decay factor explained more of the variability in dissolved Mn concentrations than the bloom factor.

K_d *values*—Our log K_d values (L kg^{-1}, mean ± SD) were 5.01 ± 0.63 for Mn, 4.68 ± 0.29 for Co, 5.21 ± 0.22 for Zn, 4.11 ± 0.51 for Cu, 4.54 ± 0.19 for Ni, and 5.93 ± 0.28 for Pb. The log K_d values for Zn were consistent with the value (~5.3 L kg^{-1}) given by Luoma et al. (1998) for spring bloom particles but higher than the value (4.52 L kg^{-1}) measured by Gee and Bruland (2002) for their South Bay samples. Gee and Bruland (2002) also measured K_d values for Ni and Cu in South Bay of 3.65 and 3.88 L kg^{-1}, respectively, which were lower than our values. However, our comparatively high K_d values were consistent with reports (Gee and Bruland 2002) of higher

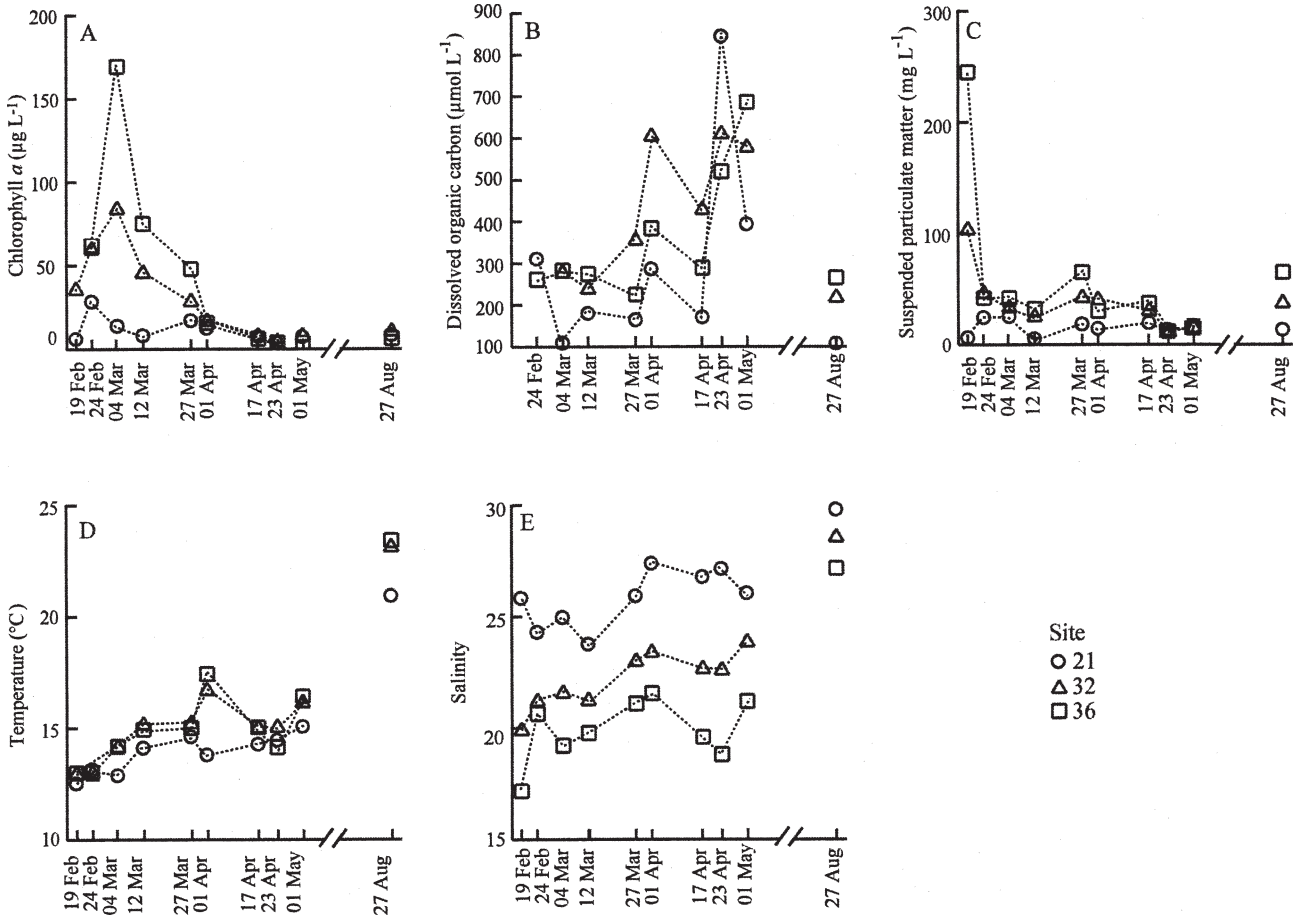

Fig. 3. Parameters measured during the spring 2003 bloom at sites 36, 32, and 21. (A) Chl *a* peaked at site 36 at >150 μg L^{-1} on 04 March. (B) DOC began to increase at the beginning of April after Chl *a* declined. Although the 23 April DOC value at site 21 was unusually high, we did not dismiss that datum because high NH_4^+ was also observed, and both observations might have been the result of wastewater treatment plant inputs. (C) SPM was high on 19 February but decreased once trace metal sampling began on 24 February. (D) Temperature and (E) salinity were relatively constant during the bloom.

K_d values in other South Bay studies and with results (Lee and Luoma 1998) that showed high algal biomass increased metal partitioning.

Models describing K_d *values*—As shown by the models in Table 6, no single factor governed the partitioning of all metals. The bloom factor explained variability in K_d values for two metals: Ni and Pb. The sorbent factor, which was partially composed of SPM, was important for only Zn and Ni partitioning. When we used partial residual plots to look at the direction of that relationship, we found a weak positive correlation between the sorbent factor and Ni, but a negative correlation for Zn. The decay factor explained some of the variability in K_d values for Zn, Ni, and Pb. For those metals, partial residual plots showed that K_d values decreased as the bloom decayed. The K_d values for Co, Cu, Ni, and Pb varied by site, with the highest values at site 21. The partitioning of many of the metals (e.g., Ni) was affected by multiple factors, which justified this statistical approach because trends were not readily apparent by looking at the raw data. Clearly, the partitioning of metals was a complex process specific to each metal.

Spring bloom conditions—The spring bloom of 2003 was one of the largest blooms on record (http://sfbay.wr.usgs.gov/access/wqdata); Chl *a* peaked at >150 μg L^{-1} at site 36 in the extreme South Bay (Fig. 3). On 19 February, before dissolved metal measurements began, there was a pulse of SPM (Fig. 3). However, by 24 February, warm, calm conditions prevailed, and SPM and salinity remained relatively constant during our sampling (Fig. 3).

By bloom peak on 04 March, DIN and DSi declined to limiting concentrations (Fig. 4). The bloom consumed 52–56 μmol L^{-1} of DIN and 75–105 μmol L^{-1} of DSi. Phytoplankton composition ratios by Brzezinski (1985) suggested that N and Si should be consumed ~1 : 1 for a diatom bloom, and the departure from this ratio indicated that N was likely recycled. DRP also declined from 6.99 and 9.91 μmol L^{-1} on 19 February to 2.65 and 3.94 μmol L^{-1} on 04 March (Fig. 4) at sites 32 and 36, respectively. However, DRP was not completely depleted as were DIN and DSi.

By 12 March, Chl *a* began declining (Fig. 3). Ammonium (NH_4^+), one indicator of bloom decay, increased at the end of April (Fig. 4). As the bloom decayed, DOC also

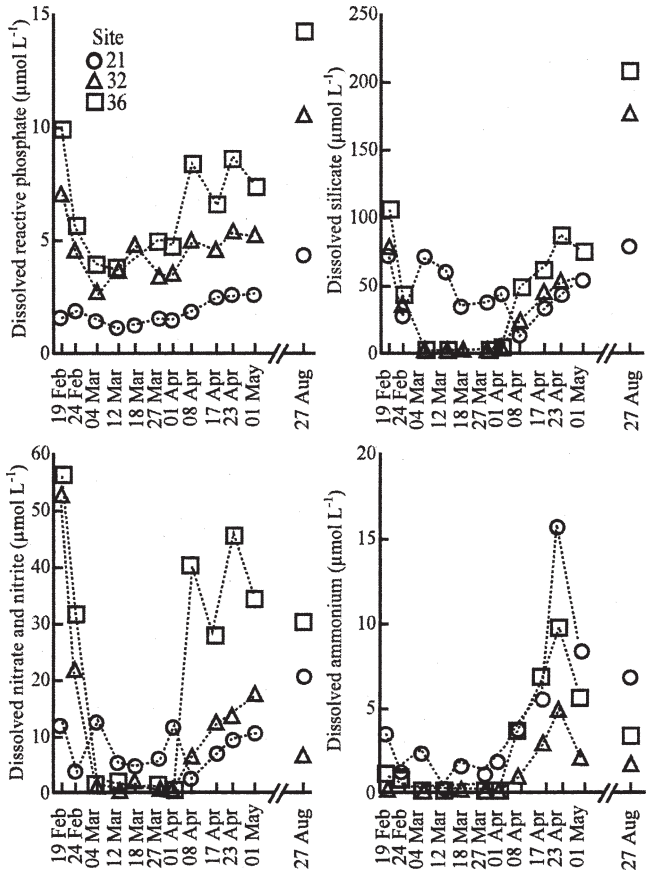

Fig. 4. Dissolved nutrients decreased during the bloom. DSi and DIN were completely depleted by the peak of the bloom on 04 March, and that depletion caused the phytoplankton to crash. Nutrient concentrations from a related USGS cruise on 18 March were added to the graphs for illustrative purposes, although those limited data were not included in the statistical analyses.

increased, beginning 01 April (Fig. 3). Finally, DOC concentrations peaked 01 May (Fig. 3).

Discussion

Role of nutrients in eutrophication—Nutrient inputs from wastewater treatment plants can contribute to the magnitude of South Bay blooms (Hager and Schemel 1996), and the blooms can in turn alter trace metal concentrations (Luoma et al. 1998). Both alterations in bloom magnitude and metal cycling are considered evidence of eutrophication (Cloern 2001). The unusually large bloom in spring 2003 was sustained by high concentrations of DIN and DSi. Figures 3 and 4 show that depletion of those nutrients lead to a crash in Chl *a*. The result was similar to findings from Hager and Schemel (1996) that showed the 1990 and 1993 blooms declined after nutrient depletion. The effect of nutrients on the bloom magnitude was our first piece of evidence for eutrophication during the 2003 bloom.

We sought to determine whether nutrient depletion coincided with trace metal drawdown, which would be further evidence of eutrophication. In contrast to nutrients, which were present at micromole per liter concentrations and depleted by up to 105 μmol L^{-1}, most trace metals measured during this study only were present at nanomole per liter concentrations, and their fractional depletion was likely to be correspondingly small (Table 1). Accordingly, we first quantitatively evaluated the potential for measuring relatively small decreases in dissolved metal concentrations.

Potential to observe changes in metal concentrations—We used known enrichment factors for metals in phytoplankton to calculate potential metal depletion during our bloom (Table 1). We then compared those values to ambient concentrations of dissolved metals to determine whether trace metal depletions could be readily observed by our experimental design. For example, phytoplankton uptake could potentially decrease dissolved Pb by 0.06 nmol L^{-1} (Table 1), a change that was reasonable to measure, given that a deviation of $\pm$0.06 described 95% of the dissolved Pb data from South Bay (0.15 $\pm$ 0.06 nmol L^{-1}) in years with intermediate freshwater inputs between 1989 and 1999 (Squire et al. 2002). In contrast, a phytoplankton depletion of dissolved Co on the order of 0.1 nmol L^{-1} (Table 1) would be difficult to detect because of the large range of Co values; only 66% of dissolved Co data for San Francisco Bay fell within 1.12 $\pm$ 0.69 nmol L^{-1} (Tovar-Sánchez et al. 2004). Thus, we expected that we would not be able to observe nutrient depletion of dissolved Co and Mn and that any measurable changes in their dissolved concentrations would be the result of other processes, particularly microbial oxidation.

We also used concentration factors (concentration per unit mass of organism/concentration per unit mass of seawater, IAEA 2004) to determine which metals were highly particle reactive and thus likely to be depleted by sorption to phytoplankton. For example, the concentration factor of Pb in phytoplankton is 10^5 (IAEA 2004), indicating that a phytoplankton bloom has the potential to remove Pb. In contrast, Ni, Co, and Zn are less particle reactive than Pb (concentration factors on the order of 10^3 to 10^4, IAEA 2004) and hence were more difficult to observe by this experimental design.

The question of whether Ni and Zn depletions could be theoretically observed was complicated by uncertainly in [metal]:[C] ratios (Table 1). For example, Twining et al. (2004) measured an order of magnitude higher [Zn]:[C] in diatoms under high iron conditions in the Southern Ocean than Bruland et al. (1991) reported for diatoms under bloom conditions in Monterey Bay on the basis of data from Martin and Knauer (1973). As a result of this uncertainty, there was an order of magnitude range in our calculated potential uptake of dissolved Zn (Table 1). For metals for which we observed algal depletion, we calculated our own [metal]:[C] ratios and compared them with previous studies. Those results are presented in the individual discussion of each metal below.

Manganese—The cycling of Mn was affected by the bloom, sorbent, and decay factors (Table 5). The bloom factor accounted for reductions in dissolved Mn concen-

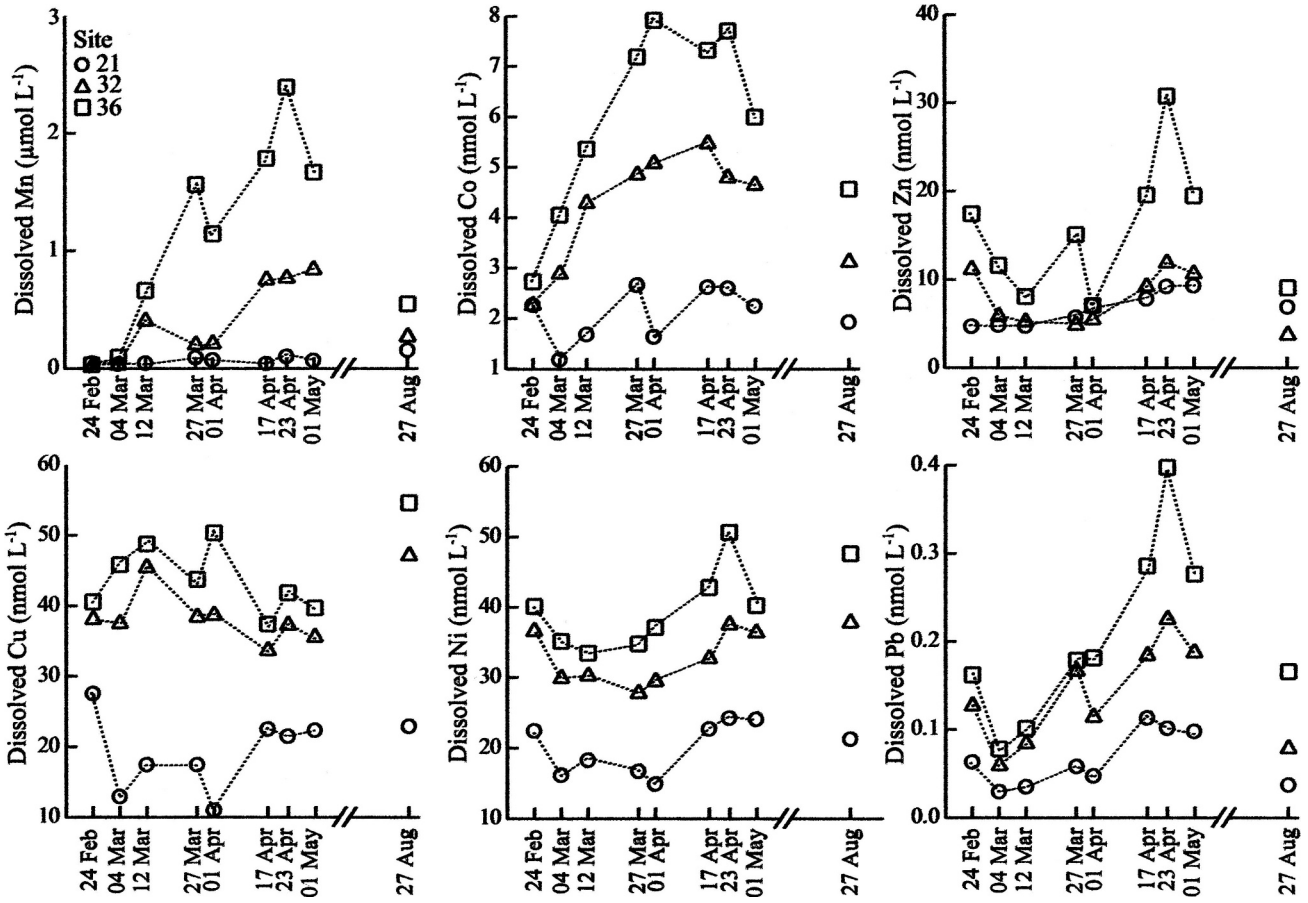

Fig. 5. Descriptive plots of dissolved trace metal concentrations during the spring 2003 bloom at sites 36, 32, and 21. These plots correspond with the plots of ancillary parameters and nutrients. For reference, Chl *a* peaked on 04 March, and DOC began to increase 01 April. To determine whether these fluctuations in dissolved metal concentrations were statistically significant, general linear models were used, and partial residual plots are presented in subsequent figures.

trations (Fig. 7). Around the time of the bloom, the number of Mn-oxidizing bacteria in the water column presumably increased as they consumed carbon generated by the bloom. Those bacteria could have decreased dissolved Mn by oxidizing soluble Mn(II) to much less soluble Mn(III) and Mn(IV).

This bacterial oxidation mechanism was proposed by Beck et al. (2002) to explain the loss of 80% of the dissolved Mn during their microcosm simulations of a South Bay bloom. Those authors investigated the cause of the Mn drawdown by adding Cu to the microcosms at concentrations that were toxic to bacteria, but not to diatoms. The resulting inhibition of Mn oxidation was evidence that Mn oxidation was bacterially mediated.

Research by Sunda and Huntsman (1987) also indicated a microbial role in Mn cycling. Those authors showed that Mn oxidation rates in seawater were too rapid to be explained by abiotic mechanisms. On the basis of these studies, we attributed most of our observed Mn depletion during the bloom to bacterial oxidation and not to nutrient uptake by diatoms, even though Mn is needed as a cofactor in photosynthetic enzymes (Morel et al. 2004).

Although the bloom factor explained a small amount of the variability in Mn concentrations (Table 5), the effect might have been greater had sampling started earlier in the season. When our sampling began in February, dissolved Mn was low: 42 and 11 nmol L^{-1} at sites 21 and 32, respectively (Fig. 5). A month before this study, concentrations of dissolved Mn were higher: 112 and 397 nmol L^{-1} at Yerba Buena Island and Dumbarton Bridge, respectively (Buck and Bruland 2005). Those sites correspond very closely our sites 21 and 32. Thus, it was likely that the sampling scheme in this study did not capture the full extent of Mn drawdown as the bloom grew.

As the bloom decomposed, dissolved Mn significantly ($p < 0.01$, Table 5) increased (Fig. 7). Dissolved Mn concentrations peaked at 2,400 nmol L^{-1} at site 36 on 23 April (Fig. 5). At that time, concentrations of particulate Mn (270 nmol L^{-1}; Fig. 6) and SPM (12 mg L^{-1}; Fig. 3) were low, indicating that the increase was not due to resuspension of sediments with high Mn concentrations. Instead, sinking and decomposition of the bloom likely reduced and released Mn from Fe and Mn (hydr)oxides in surficial sediments. When the bloom material sinks to the bottom, bacteria first use O_2 to decompose the organic material (Schoemann et al. 1998). The resulting increase in O_2 demand has been observed in sediments below South San Francisco Bay channels following a bloom (Caffrey et al.

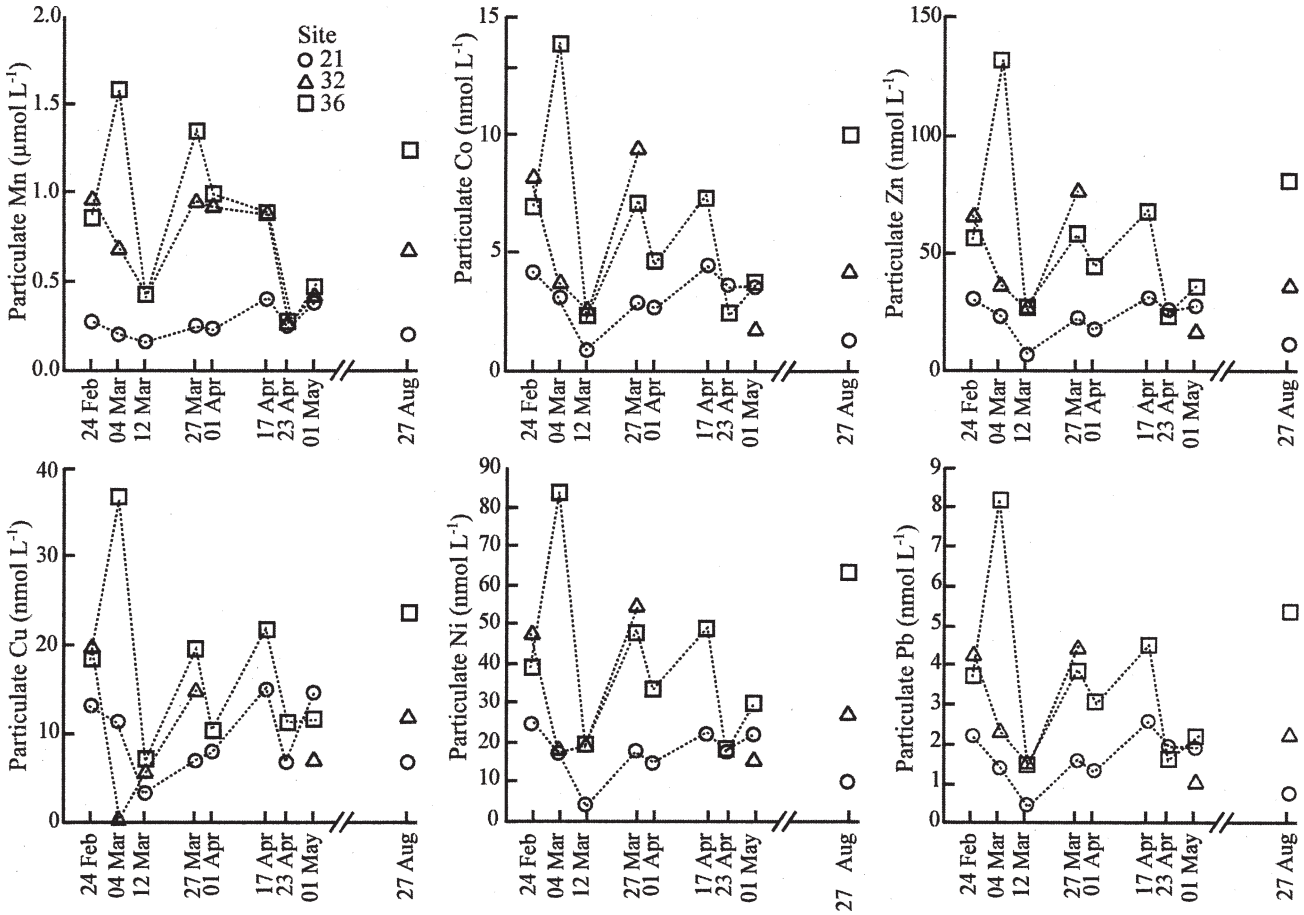

Fig. 6. Descriptive plots of particulate metal concentrations (on a per liter basis) during the spring 2003 bloom. Because most of the metals were associated with particles, minor changes in the concentration or composition of the SPM could alter the concentration of particulate metals and thus make it hard to discern the effects of the bloom. For example, at site 36, the concentration of particulate metals increased from 24 February to the peak of the bloom on 04 March, but at site 32, particulate metals decreased during that same growth period. It was unclear whether the discrepancy between sites was due to the larger magnitude of the bloom at site 36 or the loss of some components of the SPM. At site 36, the total SPM concentration (Fig. 3) did not change as the bloom grew between 24 February and 04 March, which means that the increase in bloom-derived material (Chl *a* plus Phaeo) of 14 mg L^{-1} was balanced by loss of other suspended material. During that period at site 32, bloom-derived material increased by only 2 mg L^{-1}, which did not compensate for the decrease in SPM concentrations (13 mg L^{-1}; Fig. 3). Thus, at both sites, some suspended material was lost between 24 February and 04 March. If the composition of that lost material differed between the sites, it could explain why particulate metals increased at one site but decreased at the other. Because of the difficulty in interpreting the cause of changes in particulate metal concentrations, we focused our analyses on the dissolved fraction.

1998; Grenz et al. 2000). When conditions then become suboxic, bacteria can use other elements as electron receptors, such as Mn(IV) (Beck and Bruland 2000). By reducing particulate Mn(IV) to soluble Mn(II), bacteria in suboxic conditions can increase dissolved Mn concentration (Schoemann et al. 1998; Beck and Bruland 2000).

Reduction and dissolution of Mn(IV) in suboxic sediments was the mechanism proposed by Schoemann et al. (1998) and Roitz et al. (2002) to explain increases in dissolved Mn after a phytoplankton bloom in South San Francisco Bay and in the coastal waters of the North Sea, respectively. Although Roitz et al. (2002) found that a number of different factors, including higher temperature in the summer, could contribute to fluxes of dissolved Mn from the sediments to the water, they found that intense remobilization after a phytoplankton bloom was responsible for the some of the highest concentrations of dissolved Mn. Similarly, we concluded that reduction and dissolution of Mn(IV) during bloom decomposition explained why dissolved Mn was exceptionally high in April (Fig. 5).

The following calculations also indicated that release of Mn from sediments, and not algal remineralization, was the major mechanism for the increase in dissolved Mn during April. By multiplying the increase in [C] or the decrease in [P] during the bloom by [metal]:[C] or [metal]:[P] ratios in phytoplankton, we calculated the potential amount of Mn assimilated by algae during the bloom (Table 1). We determined ΔP for sites 32 and 36 by quantifying the average decrease in DRP from 19 February to 04 March (8.45–3.29 = 5.16 μmol L^{-1}; Fig. 4). We then multiplied ΔP by the average [Mn]:[P] ratio in phytoplankton

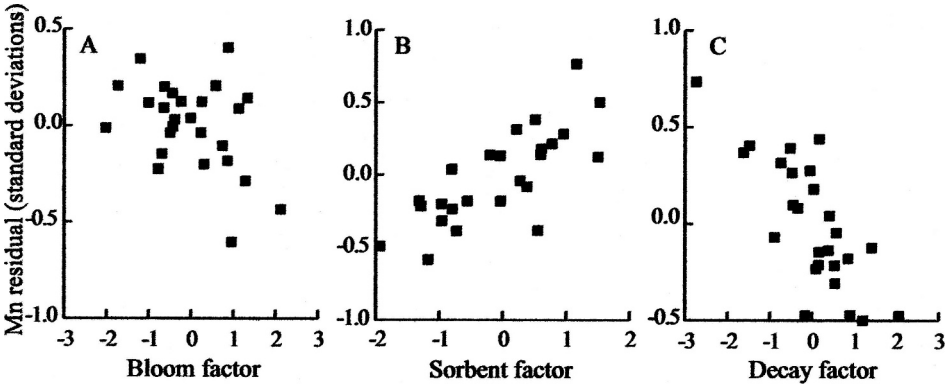

Fig. 7. Partial residual plots showing how the three PCA factors that were significant in the model (Table 5) affected dissolved Mn concentrations. (A) The bloom factor, which characterized growth of the bloom, decreased dissolved Mn concentrations. (B) Dissolved Mn concentrations increased as sorbent increased. (C) During decay, which was indicated by declining values of that factor, dissolved Mn concentrations increased. These plots display multiple linear regression results by graphing each factor on the *x*-axis versus the residuals when the model was run without that factor. The magnitude of the *y*-axis and the direction of the slope indicate the relative contribution of that factor to Mn concentrations and whether the relationship between the factor and dissolved Mn was positive or negative.

(Table 1). The resulting calculation suggested that the bloom could have at most assimilated 1.7 nmol L^{-1} of Mn:

$$\left(\frac{5.16\ \mu\text{mol P}}{\text{L}}\right)\left(\frac{0.34\ \text{mmol Mn}}{1\ \text{mol P}}\right) = \frac{1.7\ \text{nmol Mn}}{\text{L}}$$

If all 1.7 nmol L^{-1} of Mn was later remineralized from phytoplankton, it would have accounted for only 0.1% of the observed increase in dissolved Mn between 24 February and 23 April (Table 1; Fig. 5). A similar result was obtained with the use of [metal]:[C] ratios (Table 1). We concluded that remobilization from sediments likely accounted for most of the increase in dissolved Mn.

Cobalt—Cobalt cycling during the bloom differed from Mn cycling because the bloom factor did not measurably affect dissolved Co concentrations (Table 5). The difference between the two metals was unexpected. We assumed Co and Mn cycling would be linked because they are both microbially oxidized via the same pathway (Lee and Fisher 1993; Moffett and Ho 1996). According to Moffett and Ho (1996), few studies compare Mn and Co in coastal waters, but because those areas typically have high rates of microbial Mn oxidation, the two elements should have similar biogeochemistries in coastal environments. In their study of the Waquoit Bay estuary, the authors did observe one difference between the two elements: Mn oxidation was ~7× faster than Co oxidation. In our study, it was possible that differing oxidation rates explained why Mn was depleted by the bloom factor, whereas Co was not.

Alternatively, organic complexation might have blocked depletion of dissolved Co by preventing Co from being co-oxidized by Mn-oxidizing bacteria. Complexation of Co and resulting inhibition of Co oxidation was argued to be responsible for higher dissolved Co than Mn, which was not complexed, in deep waters of the Sargasso Sea (Saito and Moffett 2002).

Finally, it was possible that we did not see a decrease in dissolved Co because our sampling began too late. Although Table 1 indicated that a depletion of dissolved Co by phytoplankton was too small to measure, microbial oxidation of Co could have occurred but not been captured by our sampling scheme. Our group's previous studies, conducted as part of the Regional Monitoring Program (RMP; http://www.sfei.org/rmp/2000/2000_Annual_Results.htm and http://www.sfei.org/rmp/2001/2001_Annual_Results.htm), suggested that dissolved Co concentrations were higher when Chl *a* was <10 μg L^{-1} at the beginning of February in 2000 and 2001. During that time, dissolved Co at the Coyote Creek and Dumbarton Bridge sites, which correspond well to USGS sites 36 and 32, averaged 3.8 and 3.1 nmol L^{-1}, respectively. On the basis of the RMP data and this study, we figured that in South Bay, dissolved Co concentrations are relatively high at the beginning of February (~3.4 nmol L^{-1}), decrease before the bloom peaks (~2.5 nmol L^{-1}), exceed baseline concentrations during bloom decomposition (~6.4 nmol L^{-1}), and eventually return to baseline levels in August (~3.8 nmol L^{-1}) or even exceed those levels in some years (e.g., 2000 and 2001). Elevated Co concentrations in summer are consistent with its input from sewage discharges and remobilization from contaminated sediments in South Bay (Tovar-Sánchez et al. 2004).

Unlike the bloom factor, the decay factor significantly ($p < 0.01$; Table 5) affected dissolved Co concentrations. Dissolved Co concentrations increased as the bloom decayed (Fig. 8), largely because of reductive dissolution of Fe and Mn (hydr)oxides. Although the timing of our peak in dissolved Co (well after the Chl *a* peak; Fig. 5) was consistent with observations by Lee and Fisher (1992), showing that decaying diatoms release Co more slowly than carbon, the values in Table 1 indicate that algal reminer-

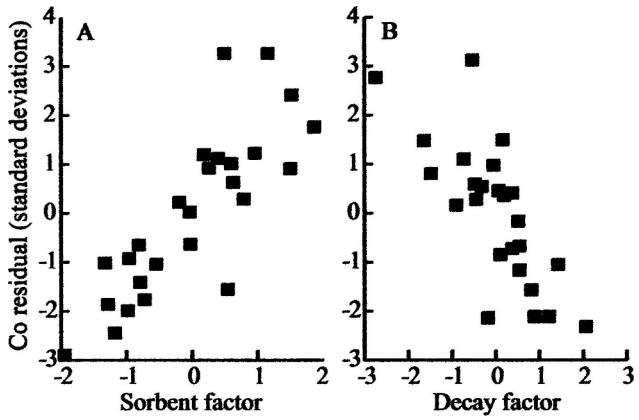

Fig. 8. Partial residual plots showing how the PCA factors that were significant in the model (Table 5) affected dissolved Co concentrations. (A) Dissolved Co concentrations significantly increased as sorbent increased. (B) During decay, which was indicated by declining values of that factor, dissolved Co concentrations increased. These plots display multiple linear regression results by running the model without one of the factors and then plotting the residuals against the omitted factor. Both the sorbent and the decay factors explained the variance in the residuals and were therefore important for determining Co concentrations.

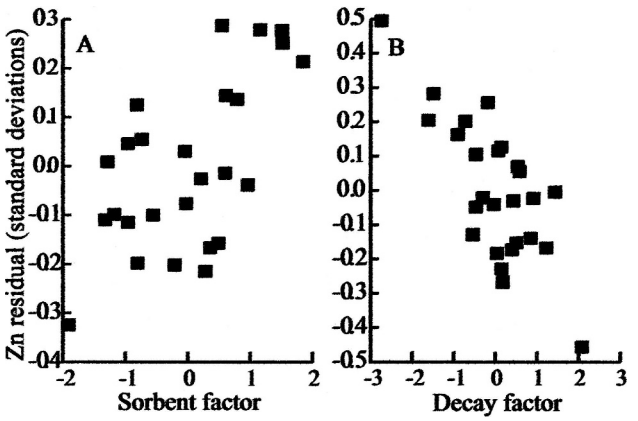

Fig. 9. Partial residual plots showing how the PCA factors that were significant in the model (Table 5) affected dissolved Zn concentrations. (A) Dissolved Zn concentrations significantly increased as sorbent increased. (B) During decay, which was indicated by declining values of that factor, dissolved Zn concentrations increased. The *y*-axis shows the residuals when the factor on the *x*-axis was omitted from the model.

alization accounted for <10% of the observed Co increase. The remainder of the increase in dissolved Co from 24 February to 01 April (Fig. 5) was likely caused by reduction and dissolution of Fe and Mn (hydr)oxides in suboxic sediments. Dissolution of Mn (hydr)oxides releases Co because it is incorporated into (hydr)oxides when bacteria co-oxidize both elements (Moffett and Ho 1996). The proposed release of Co from sediments was also consistent with the benthic remobilization observed by Rivera-Duarte and Flegal (1997). Those authors showed that for Co and Zn, concentrations were 10–100 and 1–100 (respectively) times higher in porewater than in surface water in the estuary.

Another possible explanation for the increase in dissolved Co was that high DOC in the decaying bloom caused Co to desorb from the particulate phase, but that explanation was not supported by our K_d values. Tovar-Sánchez et al. (2004) determined that desorption from the particulate phase was a major factor controlling dissolved Co concentrations in San Francisco Bay. They also found that in San Francisco Bay, Co desorbed at salinities >20. Although salinity ranged from 17 to 30 in this study, and dissolved Co as a percentage of the total did not change with salinity. The Co K_d values changed only as a function of site (Table 6). Furthermore, some of our values for dissolved Co were higher than the range of dissolved Co concentrations supported by particle desorption in Tovar-Sánchez et al. (2004). Thus, the peak that we observed in dissolved Co (Fig. 5) was tentatively attributed to diagenetic remobilization from sediments, not from Co desorption.

Zinc—Dissolved Zn was not measurably affected by the bloom factor according to our GLM (Table 5; Fig. 9). One of the advantages of using multivariate statistics to analyze the effects of the PCA factors on dissolved Zn concentrations (Table 5) is that the model measures the variation associated with a particular factor after accounting for the other terms in the model. For example, the model would have accounted for conditions, such as a pulse of SPM, which could have made a dissolved Zn depletion difficult to detect. Therefore, we were confident that the GLM (Table 5) correctly represented the sorbent and decay factors as the only two terms that affected dissolved Zn concentrations.

Furthermore, the distribution of dissolved Zn (Fig. 5) supported our statistical analyses that showed the bloom was not an important factor for describing dissolved Zn concentrations. Although the concentration of dissolved Zn at site 36 declined from the end of February to the beginning of March (Fig. 5), its concentration subsequently increased from 12 March to 27 March and then decreased to 01 April (Fig. 5). In contrast, dissolved Ni, which was significantly ($p < 0.01$; Table 5) depleted by the bloom factor, showed a steady decrease in concentration (Fig. 5).

Consequently, the factors (sorbent and decay) that affected dissolved Zn concentrations were the same as those that affected dissolved Co concentrations (Table 5) and differed from our hypothesis that phytoplankton would deplete dissolved Zn during the bloom. Phytoplankton blooms have the potential to deplete first Zn and then Co because the elements are used in the enzyme carbonic anhydrase (Morel et al. 2004). That enzyme is responsible for converting HCO_3^- to CO_2 to provide inorganic carbon during the dark reactions of the Calvin cycle.

The lack of a measurable decline in dissolved Zn concentrations in this study also differed from observations in previous field (Luoma et al. 1998; Zwolsman and van Eck 1999) and mesocosm studies (Riedel and Sanders 2003; Wang et al. 2005). In a field study of the 1994 South Bay bloom, Luoma et al. (1998) found that dissolved Zn was depleted from the water. Similarly, Zwolsman and van Eck

(1999) observed a decrease in dissolved Zn in the Scheldt estuary during a spring bloom. Mesocosm studies have confirmed those findings by adding nutrients to stimulate a bloom under controlled conditions. For example, Riedel and Sanders (2003) found that dissolved Zn was depleted in mesocosm studies with Patuxent River water, and Wang et al. (2005) showed that phytoplankton accumulated Zn from Hong Kong coastal waters. The contrasting results in our study could be because (1) sampling started too late to capture a Zn drawdown, (2) Zn was rapidly repartitioned from the particulate phase, (3) organic complexation limited Zn bioavailability, or (4) a combination of these factors.

The relationship between when sampling started and whether the metal was depleted might have been influenced by the kinetics of metal repartitioning between dissolved and particulate phases. Gee and Bruland (2002) showed that in South Bay, the Zn equilibrium between particulate and dissolved phases was established rapidly, in about 2 weeks, whereas Ni repartitioned in about 1 month. Thus, it was possible that dissolved Zn was initially depleted, but by the time this study began, Zn desorption from particulates masked any algal drawdown. The possibility that Zn was redistributed between the two phases was supported by our statistical results that showed Zn K_d values decreased with the decay factor (Table 6). A redistribution of Zn would also be consistent with its rapid desorption rates; Gee and Bruland (2002) showed that Zn desorbed more rapidly than it adsorbed (unlike Ni), and its dissolved concentration could increase by roughly 20% in a single day because of particle desorption. Therefore, in this study, Ni could have remained depleted in the water for a longer time because of its slower kinetics. Its decline was more easily observed in our experimental design.

To determine the extent to which organic complexation could have limited uptake of dissolved Zn, studies of Zn complexation in South Bay are needed. On the basis of the limited studies available (e.g., Brand et al. 1983; Sunda et al. 2005), free Zn concentrations govern growth and uptake to phytoplankton, indicating that the Zn complex might not be readily bioavailable to phytoplankton. Site-specific studies of Zn complexation in San Francisco Bay are needed because Zn complexation in estuaries is highly variable. For example, Sunda et al. (2005) showed that the amount of free Zn available for phytoplankton uptake in the Elizabeth River estuary varied by 20,000 between samples. Similarly, Kozelka and Bruland (1998), found that the percentage of complexed Zn in Narragansett Bay, Rhode Island, ranged from 51% to 97%. That complexation could be by ligands released from dying phytoplankton (Muller et al. 2005). Consequently, the sequestration of Zn in unavailable complexes could explain why it was not depleted by the bloom factor.

Both dissolved Zn and Co concentrations significantly ($p < 0.01$; Table 5) increased with the decay factor (Fig. 9). That result was consistent with previous research linking high DOC and elevated Zn in South Bay (Kuwabara et al. 1989). The possible contribution of remineralization of phytoplankton to the observed increase in dissolved Zn varied between 10% and 100%, depending which numbers were used (Table 1). However, the increase was most likely due to reductive dissolution of Fe and Mn (hydr)oxides, which have been shown (Luoma and Bryan 1981) to strongly bind Zn.

Copper—The categorical variable, site, was the most important term explaining dissolved Cu concentrations ($p < 0.01$), as demonstrated by its mean square error (Table 5). Concentrations of dissolved Cu were highest at site 36, intermediate at site 32, and lowest at site 21, which was consistent with previous research (Flegal et al. 1991). Unlike some of the other elements in this study, the decay factor was relatively unimportant for determining Cu concentrations (Table 5), and the bloom factor was not included in the model. We attributed these relatively stable dissolved Cu concentrations (Fig. 5) to complexation of dissolved Cu by organic ligands.

Previous research has demonstrated that between 80% and >99% of dissolved Cu is complexed to organic ligands in South Bay (Donat et al. 1994; Buck and Bruland 2005; Hurst and Bruland 2005). That complexation could be by (1) ligands produced by cyanobacteria (Moffett and Brand 1996), (2) natural humic and fulvic substances (Kogut and Voelker 2001), (3) synthetic chelating agents in surface or wastewater inputs (Sedlak et al. 1997), or (4) a combination of these ligands. Moreover, this complexation of Cu to strong chelating agents has been demonstrated in all seasons in South Bay (Buck and Bruland 2005).

Previous studies have demonstrated that the strong Cu complexation in South Bay limits Cu uptake to phytoplankton. Beck et al. (2002) found that >99.9% of dissolved Cu was bound to strong organic ligands in South Bay water samples collected in April 2000. According to those authors, that complexation explained why Cu was not depleted in their laboratory grow-out experiments of San Francisco Bay water isolated from benthic grazers. Similarly, Luoma et al. (1998) found that dissolved Cu was not depleted during the 1994 South Bay spring bloom. Also in a South Bay field study, Buck and Bruland (2005) found that Cu concentrations and speciation were not affected by the spring 2003 bloom.

Buck and Bruland (2005) sampled in the same year as in this study, and their data also demonstrated that dissolved Cu concentrations in January 2003 were comparable to concentrations measured here. In January, their measured dissolved Cu concentrations at Yerba Buena Island and Dumbarton Bridge were 18.9 and 33.7 nmol L^{-1}, respectively. Those values were within the range of concentrations (11.0–27.5 and 33.7–45.4 nmol L^{-1}, respectively) that we measured at our corresponding USGS sites 21 and 32 between February and May. We therefore concluded that it was unlikely that Cu depletion occurred before our first sampling date.

Copper K_d values were controlled by site-specific processes, as they were for Co. In the final model, the only variable controlling Cu K_d values was the site from which the samples were collected (Table 6). The importance of the variable site indicates that Cu partitioning was controlled by spatial factors that are not explained by the sorbent factor.

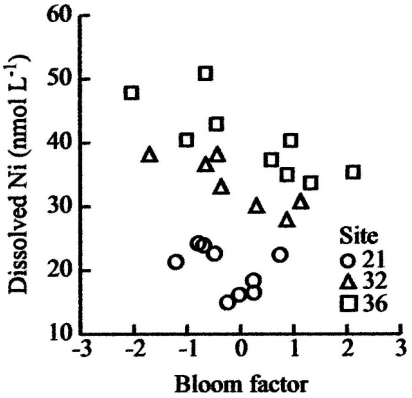

Fig. 10. Dissolved Ni concentrations were affected by both the bloom and site factors, which were significant (Table 5) factors in the Ni model. Within each site, growth of the bloom (increasing values of that factor) decreased dissolved Ni concentrations, indicating uptake by phytoplankton.

Nickel—Dissolved Ni was significantly ($p < 0.01$; Table 5) depleted by the bloom factor (Fig. 10), which followed from its role as a trace nutrient. The categorical variable, site, also significantly ($p < 0.01$; Table 5) affected dissolved Ni concentrations. Those concentrations increased from our most oceanic site to our site in the extreme South Bay (Fig. 10). In the Ni model (Table 5), the decay factor was statistically significant ($p = 0.054$; Table 5), but its comparatively low mean square error (Table 5) indicated that it accounted for only a very small amount of the variability. Thus, the two principal terms controlling Ni cycling were site and the bloom factor (Fig. 10).

The depletion of Ni during this bloom was consistent with a decrease (75% reduction) in dissolved Ni concentrations observed during the 1994 South Bay bloom (Luoma et al. 1998) but contrasted with laboratory simulations of the South Bay bloom that showed no Ni depletion (Beck et al. 2002). This discrepancy could be because of differences in the time of year the studies were conducted; seasonal changes in the relative contribution of wastewater inputs and surface runoff sources might affect the proportion of complexed Ni (Sedlak et al. 1997). About 25% of Ni surface runoff is strongly complexed by ethylenediaminetetraacetic acid (EDTA), whereas 75% of Ni in wastewater is bound to EDTA (Sedlak et al. 1997; Bedsworth and Sedlak 1999). Accordingly, in summer, when wastewater is the dominant source of freshwater to South Bay, a larger percentage of Ni is complexed by EDTA. The Beck et al. (2002) laboratory study could have contained a higher percentage of complexed Ni than in this study or the Louma et al. (1998) study because Beck and colleagues collected water in April, 2 months later than field sampling began in the other studies. Therefore, greater complexation of Ni in the Beck et al. (2002) study than in the field studies could explain why they did not observe Ni depletion.

Alternatively, the difference between the results of the studies could have been caused by UV degradation of the EDTA–Ni complex, which has been observed by Sedlak et al. (1997). UV degradation could have increased the amount of bioavailable Ni in the field relative to the Beck et al. (2002) laboratory study, which used standard fluorescent lights to culture the phytoplankton. Further field sampling and laboratory studies are needed to resolve this disparity.

We used the average increase in Chl *a* at sites 32 and 36 from 24 February to 04 March (65 μg L^{-1}) and the corresponding average decrease in dissolved Ni (5.8 nmol L^{-1}) to calculate the Ni concentration per mass of phytoplankton. We multiplied the increase in Chl *a* by the [C]:[Chl *a*] ratio (Cloern et al. 1995) and then divided by 0.3 to convert [C] to dry weight of phytoplankton (Luoma et al. 1998) as follows:

$$\left(\frac{65\ \mu\text{g Chl } a}{\text{L}}\right)\left(\frac{35\ \mu\text{g C}}{\mu\text{g Chl } a}\right)\Big/\frac{0.3\ \mu\text{g C}}{\mu\text{g phytoplankton}} = \frac{8\text{ mg phytoplankton}}{\text{L}}$$

We divided the decrease in dissolved Ni concentrations (5.8 nmol L^{-1}; Fig. 5) by the mass of phytoplankton produced (8 mg phytoplankton L^{-1}) to estimate that phytoplankton contained $\sim$0.7 μmol Ni g^{-1} dry weight. This estimate was an order of magnitude higher than concentrations of Ni in phytoplankton reported by Luoma et al. (1998) for South Bay (0.04 μmol g^{-1}) and those cited by Bruland et al. (1991) from Monterey Bay (0.05 $\pm$ 0.04 μmol g^{-1}). However, the results were more consistent with Twining et al. (2004), who reported higher [metal]:[C] ratios in phytoplankton than Bruland et al. (1991), as shown in Table 1.

Lead—The bloom factor significantly ($p < 0.01$; Table 5) depleted dissolved Pb. This depletion (Fig. 11) was presumably due to Pb sorption onto phytoplankton surfaces because Pb is highly particle reactive. The K_d values for Pb averaged $\sim 10^6$ L kg^{-1} in this study, which was consistent with previously reported K_d values ($10^{5.3}$ L kg^{-1}) for Pb in South Bay (Squire et al. 2002). The affinity of Pb for particles was also demonstrated by the order of magnitude higher Pb concentrations in the particulate phase (Fig. 6) relative to the dissolved phase (Fig. 5).

Our hypothesis that Pb was sorbed to phytoplankton was also consistent with previous calculations showing that surface area determined the Pb concentration of planktonic organisms (Michaels and Flegal 1990). Lead sorption to phytoplankton was also demonstrated in short-term laboratory experiments with Connecticut River water (Mylon et al. 2003). In those experiments, algal uptake rates of Pb spiked into Connecticut River water were not affected by temperature, indicating that most uptake was caused by binding to cell surfaces. Finally, it was unlikely that algae took up dissolved Pb internally because >95% of Pb is organically complexed in San Francisco Bay (Kozelka et al. 1997).

We calculated the Pb concentration per mass of phytoplankton following the same method we used to calculate the Ni concentration in phytoplankton. We

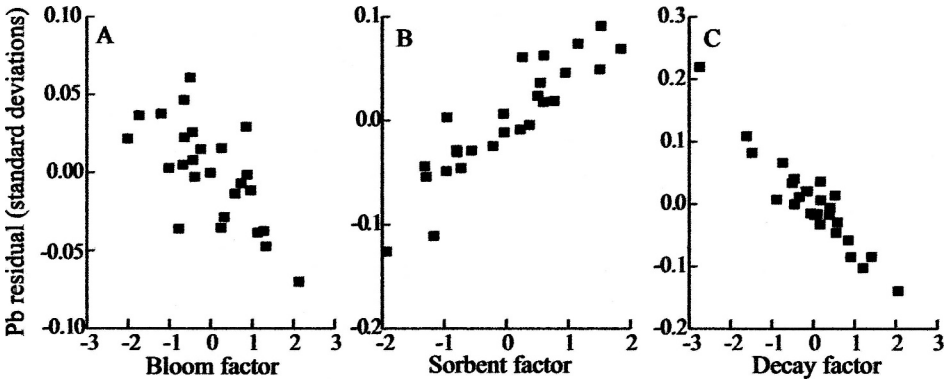

Fig. 11. Partial residual plots showing how the three PCA factors that were significant in the model (Table 5) affected dissolved Pb concentrations. (A) Dissolved Pb concentrations decreased during the bloom. (B) Dissolved Pb concentrations increased as sorbent increased. (C) During decay, which was indicated by declining values of that factor, dissolved Pb concentrations increased. The plots show the residuals when the model was run with two of the three factors versus the remaining factor on the *x*-axis. The residuals on the *y*-axis are shown in terms of standard deviations. Accordingly, decay, which explained large standard deviations in the residuals, was more important to the model than bloom.

divided the decrease in dissolved Pb (0.08 nmol L^{-1}; Fig. 5) from 24 February to 04 March at sites 32 and 36 by the mass of phytoplankton produced (8 mg phytoplankton L^{-1}) during that time to determine that phytoplankton contained 0.01 μmol Pb g^{-1} dry weight. That estimated concentration was consistent with the single detectable value for Pb in phytoplankton (0.01 μmol Pb g^{-1}) with low Al ($<$100 μg g^{-1}; *see* Bruland et al. 1991) reported by Martin and Knauer (1973). Similarly, in the Seine estuary, Pb concentrations in diatoms were 0.07 μmol Pb g^{-1} (Miramand et al. 1998). Our results were also consistent with culture studies that showed phytoplankton could accumulate up to 1.7×10^4 more Pb per cell volume than in an equivalent amount of ambient water, and that the uptake was associated with the cell walls (Fisher et al. 1983). Finally, by scavenging Pb, the bloom could help retain that metal within the estuary, as has been observed for other metals (Luoma et al. 1998).

Although the bloom factor accounted for depletion of dissolved Pb concentrations, the most important factor affecting dissolved Pb concentrations was the decay factor (Table 5). During decomposition of the bloom, which was indicated by decreasing values of the decay factor, dissolved Pb concentrations increased (Table 5; Fig. 11). The increase in dissolved Pb was consistent with the diagenetic release of Pb from historically contaminated sediments, which are now the major source of Pb to San Francisco Bay waters (Steding et al. 2000; Flegal et al. 2005).

Annual contribution of phytoplankton—We calculated the amount of Ni from wastewater treatment plants that was cycled through phytoplankton annually to determine whether phytoplankton could be an important mechanism for trapping anthropogenically derived metals in the estuary. We focused on the region of the South Bay south of the Dumbarton Bridge (lower South Bay) because our sites 32 and 36 bracketed that area (Fig. 1). Following calculations in Luoma et al. (1998), we calculated the ratio of metal depleted (ΔMetal) to DRP depleted (ΔDRP) for the period between 24 February and 04 March.

$$\gamma_{\text{Metal}} = \frac{\Delta\text{Metal}}{\Delta\text{DRP}} = \frac{5.8 \text{ nmol L}^{-1}}{1{,}750 \text{ nmol L}^{-1}} = 3.3 \times 10^{-3}$$

We then determined the annual DRP consumption, according to

$$\left(\frac{12.5 \text{ mol C}}{\text{m}^2} \text{ net production}\right)\left(3.4 \times 10^7 \text{ m}^2 \text{ surface area}\right)\left(\frac{1 \text{ mol P}}{106 \text{ mol C}}\right) = 4.0 \times 10^6 \text{ mol P yr}^{-1}$$

where the product of the annual South Bay net production (Cole and Cloern 1984) and the lower South Bay surface area (Hager and Schemel 1996) gave the South Bay annual primary production, and division by the Redfield ratio converted the annual C production to annual P consumption. Then, we multiplied the annual P consumption by γ_{Metal} and found that algae in lower South Bay have the potential to sorb (adsorb or assimilate) 1.3×10^4 mol of Ni each year.

The 1.3×10^4 mol of Ni cycled by the phytoplankton was about 75% of the Ni discharged into the lower South Bay by wastewater treatment plants in 2003. In that year, the Palo Alto, San Jose and Santa Clara, and Sunnyvale wastewater treatment plants released 1.8×10^4 mol of Ni to the lower South Bay (R. E. Looker pers. comm.). The trapping of discharged Ni by phytoplankton was consistent with results from Luoma et al. (1998), which showed that about 60% of the Ni discharged to the entire South Bay was assimilated by phytoplankton. As those authors discussed, these calculations were rough because [metal]:[P] uptake ratios by phytoplankton vary. Furthermore, our calculation of Ni assimilation was conservative because we used the primary productivity calculated for South Bay, not the

lower South Bay where blooms are more intense. Despite these uncertainties, we concluded that (1) Ni loadings to South Bay from wastewater treatment plants are relatively large, (2) phytoplankton trap enough Ni that changes in phytoplankton biomass will affect metal cycling and retention, and (3) the bloom has the potential to introduce Ni to the food chain because benthic organisms often take advantage of the bloom to grow and reproduce (Thompson and Nichols 1988).

Phytoplankton play an important role in metal cycling in the estuary by trapping metals, making those metals bioavailable to the food chain, and altering metal concentrations during bloom events. Accordingly, changes in phytoplankton biomass (e.g., from nutrient enrichment) are likely to have complex effects on metal cycling that might not be readily anticipated. That conclusion is consistent with models by Cloern (2001) that show eutrophication has unique and subtle manifestations in each estuary, including alterations in metal cycling in the San Francisco Bay.

By exploiting the predictability of the South Bay bloom, we were able to determine which metals were affected by nutrient-enriched blooms. Only 3 of the metals in this study (Mn, Ni, and Pb) were decreased by the bloom factor (Table 5). During the bloom, Ni was likely assimilated by phytoplankton and made bioavailable to the food chain. Contrary to our hypotheses, dissolved Co and Zn were not measurably depleted by the bloom factor, possibly because (1) sampling started too late to capture the drawdown, (2) kinetics of oxidation and repartitioning masked the depletions, (3) organic complexation limited the bioavailability of the metals, or (4) a combination of these factors. Consistent with our hypothesis, dissolved Cu was not affected by either the bloom or decay factors, attesting to its strong organic complexation that limits its bioavailability and toxicity in the estuary. The decay of the bloom material also affected cycling of other metals. Dissolved Mn, Co, Zn, and Pb were remobilized, presumably by reductive dissolution of Fe and Mn (hydr)oxides in surficial sediments during algal decomposition. The effects of the bloom and its decay on metal concentrations in the estuary were consistent with the biogeochemistries of the metals and demonstrated that nutrient-enriched blooms affect metal cycling.

References

Beck, N. G., and K. W. Bruland. 2000. Diel biogeochemical cycling in a hyperventilating shallow estuarine environment. Estuaries **23:** 177–187.

———, ———, and E. L. Rue. 2002. Short-term biogeochemical influence of a diatom bloom on the nutrient and trace metal concentrations in South San Francisco Bay microcosm experiments. Estuaries **25:** 1063–1076.

Bedsworth, W. W., and D. L. Sedlak. 1999. Sources and environmental fate of strongly complexed nickel in estuarine waters: The role of ethylenediaminetetraacetate. Environ. Sci. Technol. **33:** 926–931.

Brand, L. E., W. G. Sunda, and R. R. L. Guillard. 1983. Limitation of marine phytoplankton reproductive rates by zinc, manganese, and iron. Limnol. Oceanogr. **28:** 1182–1198.

Bruland, K. W., J. R. Donat, and D. A. Hutchins. 1991. Interactive influences of bioactive trace metals on biological production in oceanic waters. Limnol. Oceanogr. **36:** 1555–1577.

———, and M. C. Lohan. 2004. Controls of trace metals in seawater. Treatise Geochem. **6:** 23–47.

Brzezinski, M. A. 1985. The Si : C : N ratio of marine diatoms: Interspecific variability and the effect of some environmental variables. J. Phycol. **21:** 347–357.

Buck, K. N., and K. W. Bruland. 2005. Copper speciation in San Francisco Bay: A novel approach using multiple analytical windows. Mar. Chem. **96:** 185–198.

Caffrey, J. M., J. E. Cloern, and C. Grenz. 1998. Changes in production and respiration during a spring phytoplankton bloom in San Francisco Bay, California, USA: Implications for net ecosystem metabolism. Mar. Ecol. Prog. Ser. **172:** 1–12.

Cloern, J. E. 1996. Phytoplankton bloom dynamics in coastal ecosystems: A review with some general lessons from sustained investigation of San Francisco Bay, California. Rev. Geohpys. **34:** 127–168.

———. 2001. Our evolving conceptual model of the coastal eutrophication problem. Mar. Ecol. Prog. Ser. **210:** 223–253.

———, and R. Dufford. 2005. Phytoplankton community ecology: Principles applied in San Francisco Bay. Mar. Ecol. Prog. Ser. **285:** 11–28.

———, C. Grenz, and L. Vidergar-Lucas. 1995. An empirical model of the phytoplankton chlorophyll : carbon ratio—the conversion factor between productivity and growth rate. Limnol. Oceanogr. **40:** 1313–1321.

Cole, B. E., and J. E. Cloern. 1984. Significance of biomass and light availability to phytoplankton productivity in San Francisco Bay. Mar. Ecol. Prog. Ser. **17:** 15–24.

Donat, J. R., K. A. Lao, and K. W. Bruland. 1994. Speciation of dissolved copper and nickel in South San Francisco Bay: A multi-method approach. Anal. Chim. Acta **284:** 547–571.

Fisher, N. S., K. A. Burns, R. D. Cherry, and M. Heyraud. 1983. Accumulation and cellular distribution of ^{241}Am, ^{210}Po, and ^{210}Pb in two marine algae. Mar. Ecol. Prog. Ser. **11:** 233–237.

Flegal, A. R., C. H. Conaway, G. M. Scelfo, S. A. Hibdon, and S. A. Sañudo-Wilhelmy. 2005. A review of factors influencing measurements of decadal variations in metal contamination in San Francisco Bay, California. Ecotoxicology **14:** 645–660.

———, G. J. Smith, G. A. Gill, S. Sañudo-Wilhelmy, and L. C. D. Anderson. 1991. Dissolved trace element cycles in the San Francisco Bay estuary. Mar. Chem. **36:** 329–363.

Gee, A. K., and K. W. Bruland. 2002. Tracing Ni, Cu, and Zn kinetics and equilibrium partitioning between dissolved and particulate phases in South San Francisco Bay, California, using stable isotopes and high-resolution inductively coupled plasma mass spectrometry. Geochim. Cosmochim. Acta **66:** 3063–3083.

Granéli, W., and E. Granéli. 1991. Automatic potentiometric determination of dissolved oxygen. Mar. Biol. **108:** 341–348.

Grenz, C., J. E. Cloern, S. W. Hager, and B. E. Cole. 2000. Dynamics of nutrient cycling and related benthic nutrient and oxygen fluxes during a spring phytoplankton bloom in South San Francisco Bay (USA). Mar. Ecol. Prog. Ser. **197:** 67–80.

Hager, S. W. 1994. Dissolved nutrient and suspended particulate matter data for the San Francisco Bay estuary, California, October 1991 through November 1993. U.S. Geol. Surv. open-file report 94-471.

———, AND L. E. SCHEMEL. 1996. Dissolved inorganic nitrogen, phosphorus and silicon in South San Francisco Bay I. Major factors affecting distributions. *In* J. T. Hollibaugh [ed.], San Francisco Bay, The ecosystem: Further investigations into the natural history of San Francisco Bay and Delta with reference to the influence of man. Pacific Division of the American Association for the Advancement of Science.

HURST, M. P., AND K. W. BRULAND. 2005. The use of Nafion-coated thin mercury film electrodes for the determination of the dissolved copper speciation in estuarine water. Anal. Chim. Acta **546:** 68–78.

[IAEA] INTERNATIONAL ATOMIC ENERGY AGENCY. 2004. Sediment distribution coefficients and concentration factors for biota in the marine environment. Tech. Rep. Ser. 422, IAEA.

INGRI, J., AND OTHERS. 2004. Size distribution of colloidal trace metals and organic carbon during a coastal bloom in the Baltic Sea. Mar. Chem. **91:** 117–130.

KOGUT, M. B., AND B. M. VOELKER. 2001. Strong copper-binding behavior of terrestrial humic substances in seawater. Environ. Sci. Technol. **35:** 1149–1156.

KOZELKA, P. B., AND K. W. BRULAND. 1998. Chemical speciation of dissolved Cu, Zn, Cd, Pb in Narragansett Bay, Rhode Island. Mar. Chem. **60:** 267–282.

———, S. SANUDO-WILHELMY, A. R. FLEGAL, AND K. W. BRULAND. 1997. Physico-chemical speciation of lead in South San Francisco Bay. Estuar. Coast. Shelf Sci. **44:** 649–658.

KUWABARA, J. S., C. C. Y. CHANG, J. E. CLOERN, T. L. FRIES, J. A. DAVIS, AND S. N. LUOMA. 1989. Trace metal associations in the water column of South San Francisco Bay, California. Estuar. Coast. Shelf Sci. **28:** 307–326.

LEE, B.-G., AND N. S. FISHER. 1992. Degradation and elemental release rates from phytoplankton debris and their geochemical implications. Limnol. Oceanogr. **37:** 1345–1360.

———, AND ———. 1993. Microbially mediated cobalt oxidation in seawater revealed by radiotracer experiments. Limnol. Oceanogr. **38:** 1593–1602.

———, AND S. N. LUOMA. 1998. Influence of microalgal biomass on absorption efficiency of Cd, Cr, and Zn by two bivalves from San Francisco Bay. Limnol. Oceanogr. **43:** 1455–1466.

LUOMA, S. N., AND G. W. BRYAN. 1981. A statistical assessment of the form of trace metals in oxidized estuarine sediments employing chemical extractants. Sci. Total Environ. **17:** 165–196.

———, A. VAN GEEN, B.-G. LEE, AND J. E. CLOERN. 1998. Metal uptake by phytoplankton during a bloom in South San Francisco Bay: Implications for metal cycling in estuaries. Limnol. Oceanogr. **43:** 1007–1016.

MARTIN, J. H., AND G. A. KNAUER. 1973. The elemental composition of plankton. Geochim. Cosmochim. Acta **37:** 1639–1653.

MICHAELS, A. F., AND A. R. FLEGAL. 1990. Lead in marine planktonic organisms and pelagic food webs. Limnol. Oceanogr. **35:** 287–295.

MIRAMAND, P., D. FICHET, D. BENTLEY, J.-C. GUARY, AND F. CAURANT. 1998. Heavy metal concentrations (Cd, Cu, Pb, Zn) at different levels of the pelagic trophic web collected along the gradient of salinity in the Seine estuary. Earth Planet. Sci. **327:** 259–264.

MOFFETT, J. W., AND L. E. BRAND. 1996. Production of strong, extracellular Cu chelators by marine cyanobacteria in response to Cu stress. Limnol. Oceanogr. **41:** 388–395.

———, AND J. HO. 1996. Oxidation of cobalt and manganese in seawater via a common microbially catalyzed pathway. Geochim. Cosmochim. Acta **60:** 3415–3424.

MOREL, F. M. M., AND J. G. HERING. 1993. Principles and applications of aquatic chemistry. Wiley.

———, A. J. MILLIGAN, AND M. A. SAITO. 2004. Marine bioinorganic chemistry. The role of trace metals in the oceanic cycles of major nutrients. Treatise Geochem. **6:** 113–143.

MULLER, F. L. L., A. LARSEN, C. A. STEDMON, AND M. SONDERGAARD. 2005. Interactions between algal–bacterial populations and trace metals in fjord surface waters during a nutrient-stimulated summer bloom. Limnol. Oceanogr. **50:** 1855–1871.

MYLON, S. E., B. S. TWINING, N. S. FISHER, AND G. BENOIT. 2003. Relating the speciation of Cd, Cu, and Pb in two Connecticut rivers with their uptake in algae. Environ. Sci. Technol. **37:** 1261–1267.

NDUNG'U, K., R. P. FRANKS, K. W. BRULAND, AND A. R. FLEGAL. 2003. Organic complexation and total dissolved trace metal analysis in estuarine waters: Comparison of solvent-extraction graphite furnace atomic absorption spectrometric and chelating resin flow injection inductively coupled plasma–mass spectrometric analysis. Anal. Chim. Acta **481:** 127–138.

OSENBERG, C. W., R. J. SCHMITT, S. J. HOLBROOK, AND D. CANESTRO. 1992. Spatial scale of ecological effects associated with an open coast discharge of produced water. Environ. Sci. Res. **46:** 387–402.

PARSONS, T. R., Y. MAITA, AND C. M. LALLI. 1984. A manual of chemical and biological methods for seawater analysis, 1st ed. Pergamon.

RIEDEL, G. F., AND J. G. SANDERS. 2003. The interrelationships among trace element cycling, nutrient loading, and system complexity in estuaries: A mesocosm study. Estuaries **26:** 339–351.

RIVERA-DUARTE, I., AND A. R. FLEGAL. 1997. Porewater gradients and diffusive benthic fluxes of Co, Ni, Cu, Zn, and Cd in San Francisco Bay. Croat. Chem. Acta **70:** 389–417.

ROITZ, J. S., A. R. FLEGAL, AND K. W. BRULAND. 2002. The biogeochemical cycling of manganese in San Francisco Bay: Temporal and spatial variations in surface water concentrations. Estuarine, Coastal and Shelf Science **54:** 227–239.

SAITO, M. A., AND J. W. MOFFETT. 2002. Temporal and spatial variability of cobalt in the Atlantic Ocean. Geochim. Cosmochim. Acta **66:** 1943–1953.

SCHOEMANN, V., H. J. W. DE BAAR, J. T. M. DE JONG, AND C. LANCELOT. 1998. Effects of phytoplankton blooms on the cycling of manganese and iron in coastal waters. Limnol. Oceanogr. **43:** 1427–1441.

SEDLAK, D. L., J. T. PHINNEY, AND W. W. BEDSWORTH. 1997. Strongly complexed Cu and Ni in wastewater effluents and surface runoff. Environ. Sci. Technol. **31:** 3010–3016.

SHARP, J. H., R. BENNER, L. BENNETT, C. A. CARLSON, R. DOW, AND S. E. FITZWATER. 1993. Re-evaluation of high temperature combustion and chemical oxidation measurements of dissolved organic carbon in seawater. Limnol. Oceanogr. **38:** 1774–1782.

SQUIRE, S., G. SCELFO, M. J. REVENAUGH, AND A. R. FLEGAL. 2002. Decadal trends of silver and lead contamination in San Francisco Bay surface waters. Environ. Sci. Technol. **36:** 2379–2386.

STEDING, D. J., C. E. DUNLAP, AND A. R. FLEGAL. 2000. New isotopic evidence for chronic lead contamination in the San Francisco Bay estuary system: Implications for the persistence of past industrial lead emissions in the biosphere. Proc. Natl. Acad. Sci. USA **97:** 11181–11186.

SUNDA, W. G., J. R. DONAT, S. A. HUNTSMAN, AND G. CARRASCO. 2005. Control of zinc uptake by estuarine plankton by free zinc ion concentration (abstract). The American Society of Limnology and Oceanography Aquatic Sciences Meeting. Salt Lake City, 20–25 February.

———, AND S. A. HUNTSMAN. 1987. Microbial oxidation of manganese in a North Carolina estuary. Limnol. Oceanogr. **32:** 552–564.

———, AND ———. 1988. Effect of sunlight on redox cycles of manganese in the southwestern Sargasso Sea. Deep-Sea Res. Part 1 Oceanogr. Res. Pap. **35:** 1297–1317.

———, AND ———. 1998. Processes regulating cellular metal accumulation and physiological effects: Phytoplankton as model systems. Sci. Total Environ. **219:** 165–181.

TABACHNICK, B. G., AND L. S. FIDELL. 2001. Using multivariate statistics, 4th ed. Allyn and Bacon.

THAMDRUP, B., H. FOSSING, AND B. B. JØRGENSEN. 1994. Manganese, iron, and sulfur cycling in a coastal marine sediment, Aarhus Bay, Denmark. Geochim. Cosmochim. Acta **58:** 5115–5129.

THOMPSON, J. K., AND F. H. NICHOLS. 1988. Food availability controls seasonal cycle of growth in *Macoma Balthica* (L.) in San Francisco Bay, California. J. Exp. Mar. Biol. Ecol. **116:** 43–62.

TOVAR-SÁNCHEZ, A., S. A. SAÑUDO-WILHELMY, AND A. R. FLEGAL. 2004. Temporal and spatial variations in the biogeochemical cycling of cobalt in two urban estuaries: Hudson River estuary and San Francisco Bay. Estuar. Coast. Shelf Sci. **60:** 717–728.

TWINING, B. S., S. B. BAINES, AND N. S. FISHER. 2004. Element stoichiometries of individual plankton cells collected during the Southern Ocean iron experiment (SOFeX). Limnol. Oceanogr. **49:** 2115–2128.

WANG, W. X., R. C. H. DEI, AND H. S. HONG. 2005. Seasonal study on the Cd, Se, and Zn uptake by natural coastal phytoplankton assemblages. Environ. Toxicol. Chem. **24:** 161–169.

WARNKEN, K. W., D. TANG, G. A. GILL, AND P. H. SANTSCHI. 2000. Performance optimization of a commercially available iminodiacetate resin for the determination of Mn, Ni, Cu, Cd and Pb by on-line preconcentration inductively coupled plasma–mass spectrometry. Anal. Chim. Acta **423:** 265–276.

ZWOLSMAN, J. J. G., AND G. T. M. VAN ECK. 1999. Geochemistry of major elements and trace metals in suspended matter of the Scheldt estuary, southwest Netherlands. Mar. Chem. **66:** 91–111.

Received: 4 January 2006
Accepted: 19 September 2006
Amended: 29 November 2006